Available online at www.sciencedirect.com
ScienceDirect
Journal of Geodynamics 42 (2006) 115–139
JOURNAL OF GEODYNAMICS
http://www.elsevier.com/locate/jog

Neogene volcanic activity of western Syria and its relationship with Arabian plate kinematics ☆

Michele Lustrino [a,b,*], Evgenii Sharkov [c]

[a] *Dipartimento di Scienze della Terra, Università degli Studi di Roma La Sapienza, P.le A. Moro 5, 00185 Roma, Italy*
[b] *Istituto di Geologia Ambientale e Geoingegneria (IGAG-CNR), c/o Dipartimento di Scienze della Terra, Università degli Studi di Roma La Sapienza, P.le A. Moro 5, 00185 Roma, Italy*
[c] *Institute of Geology of Ore Deposits, Petrography, Mineralogy and Geochemistry (IGEM), Russian Academy of Sciences, Staromonetnyi per. 35, Moscow, 119017 Russia*

Received 25 January 2006; received in revised form 1 June 2006; accepted 8 June 2006

Abstract

The Cenozoic (mostly Neogene) volcanic activity in Syria is part of the extensive magmatism that took place in the Mashrek Region, Middle East, from upper Eocene to Holocene (~40–0.0005 Ma). Samples in western Syria are mostly high TiO_2 (TiO_2 ~1.8–3.7 wt.%) alkaline mafic rocks (basanites, hawaiites and alkali basalts) plus rare transitional/tholeiitic basalts and basaltic andesites) with within-plate-like trace element signature.

On the basis of incompatible trace element content, the volcanic activity in Syria has been divided into two stages: the first lasting from ~25 to ~5 Ma and the second from ~5 to recent times. Indeed, the Syrian lavas show incompatible trace element content increasing with decreasing age from ~25 to ~5 Ma, followed by an abrupt decrease to low values roughly at the Miocene–Pliocene boundary. This temporal shift in composition is related to major tectonic re-organization occurred during upper Miocene.

The proposed petrogenetic model invokes three steps: (a) passive upwelling of the shallow asthenosphere during the development of the Dead Sea transform fault system. Different degrees of partial melting were followed by variable extents of fractional crystallization and limited upper crustal contamination; (b) the Miocene–Pliocene boundary tectonic change enhanced passive decompression of the same sources and a consequent increase in degree of partial melting resulting in low incompatible trace element content of the relatively high-volume liquids; (c) after this phase, the incompatible trace element content in the basaltic magmas increased as consequence of fractional crystallization processes.

Major and trace element content similarities with the rest of the circum-Mediterranean igneous rocks are consistent with a common relatively shallow origin for the Cenozoic anorogenic magmatism of the entire circum-Mediterranean area (the so-called Common Magmatic Reservoir). Because much of the igneous activity in the studied area is concentrated near the Dead Sea fault, the origin of Cenozoic magmatism in Syria (and in the rest of the circum-Mediterranean area) reflects a strong lithospheric control on the loci of partial melting. Mantle plumes from lower mantle and/or north-westward channelling of the Afar mantle plume is not needed to explain volcanic activity in Syria and the Mashrek area.

Keywords: Syria; Arabia; Basalt; Neogene; Plume; CiMACI; Petrology; Lithosphere

☆ Paper presented at the 5th Forum Geoitalia 2005, Spoleto, Italy.

* Corresponding author. Tel.: +39 6 49914158; fax: +39 6 4454729.
E-mail address: michele.lustrino@uniroma1.it (M. Lustrino).

0264-3707/$ – see front matter © 2006 Elsevier Ltd. All rights reserved.
doi:10.1016/j.jog.2006.06.003

1. Introduction

Circum-Mediterranean Cenozoic igneous rocks comprise an extremely wide range of chemical compositions (e.g., Lustrino, 2000, 2003; Wilson and Bianchini, 1999; Lustrino and Wilson, in press; Beccaluva et al., in press) with "anorogenic" and "orogenic" geochemical characteristics (see Lustrino and Wilson, in press for a proposed definition of "anorogenic" and "orogenic"). Amongst these products, the volcanic rocks of Syria have not been thoroughly studied. Indeed, with the exception of few geochronological studies (e.g., Mouty et al., 1992; Sharkov et al., 1994, 1998), a geochemical and petrological modelling for the Cenozoic igneous rocks of Syria is lacking. Recently, the scientific community has shown some interest on the Cenozoic volcanic rocks of Mashrek (Middle East), however confined to areas surrounding Syria (e.g., SE Turkey, Jordan, Lebanon, Israel; Stein and Hofmann, 1992; Polat et al., 1997; Weinstein, 2000; Alici et al., 2001; Ilani et al., 2001; Bertrand et al., 2003; Ibrahim et al., 2003; Shaw et al., 2003; Abdel-Rahman and Nassa, 2004; Weinstein et al., 2006).

Syrian Cenozoic volcanic rocks are important for several reasons: (a) Cenozoic volcanism in Syria occurs in a complex geodynamic setting, near a continental margin (easternmost Mediterranean Sea) between the Levantine subplate (part of the African Plate) and the Arabian Plate, separated by a major strike-slip fault (the Dead Sea Transform; hereafter DST); (b) in the Mashrek, important volcanic activity developed during the Cenozoic, with huge plateaux of basaltic lava whose origin has been related to mantle plumes (active upwelling of sub-lithospheric mantle) or to lithospheric–asthenospheric passive upwelling (see discussion in Lustrino and Wilson, in press); (c) the igneous activity in Syria and neighbouring areas is associated with asymmetric uplift of the DST, with the eastern continental shoulder about 1 km more elevated than the western counterpart. This asymmetry, continuing southward to the Red Sea, has been related to channelling of the Afar mantle plume from the south (e.g., Sobolev et al., 2005); (d) mantle xenoliths associated with Syrian alkaline lavas provide direct evidence about the nature of the subcontinental lithospheric mantle; (e) together with Hyblean Mts. in Sicily, Mashrek is the only place in the circum-Mediterranean area characterized by a very prolonged igneous activity dating back at least to Jurassic times with relatively homogeneous geochemical composition (e.g., mildly alkaline sodic basalts to tholeiitic basalts with "anorogenic" geochemical characteristics; see discussion in Lustrino and Wilson, in press).

The aims of this paper are: (1) to characterize representative volcanic rocks from Syria; (2) to evaluate variation in composition of basaltic melts with age during the Cenozoic; (3) compare these products with other Cenozoic volcanic rocks from Mashrek area and with the "anorogenic" volcanic rocks from the rest of the circum-Mediterranean area; (4) to place constraints on the relative role of lithospheric and sub-lithospheric mantle sources; (5) to decipher the main causes for the origin of the volcanic activity in this area (e.g., passive or active upwelling of mantle).

The Syrian Cenozoic volcanic rocks are here modelled as the products of partial melting of shallow mantle (lowermost lithospheric mantle or shallow asthenosphere) with a variable spinel/garnet ratio without influence from the nearby Afar mantle plume. The absence of strong uplift (doming), the low heat flow measured in the area, the absence of age progression of magmatism and some subtle geochemical differences between Mashrek and Afar plume-related volcanic rocks are inconsistent with a model involving any role of the Afar plume. A major change in plate kinematics is believed to be the cause of an abrupt increase of partial melting at the Miocene–Pliocene boundary. The relative constancy of incompatible trace element ratios (but associated with relatively large differences in incompatible trace element abundance) in lavas emplaced during the last ~25 Ma can be interpreted as an evidence for common mantle sources and relatively minor upper crustal contamination processes.

2. Geological background

The Levantine Basin represents the south easternmost sector of the Mediterranean Sea (Fig. 1). Its origin has been related to the opening of the Neo-Tethys and its composition is now considered to be thinned continental crust (e.g., Netzeband et al., 2006). Geological and geophysical data show that the Levantine crust is mostly made up of ~10 km thick Phanerozoic sedimentary successions (mostly carbonates) overlying a transitional igneous–metamorphic basement ~12 km thick (e.g., Ben-Avraham and Ginzburg, 1990; Khair and Tsokas, 1999; Aksu et al., 2005; Netzeband et al., 2006). During the Mesozoic, passive continental margin-related igneous activity occurred at several localities (e.g., Mouty et al., 1992; Stein and Hofmann, 1992; Abdel-Rahman, 2002). Picritic to alkali basalts occur between

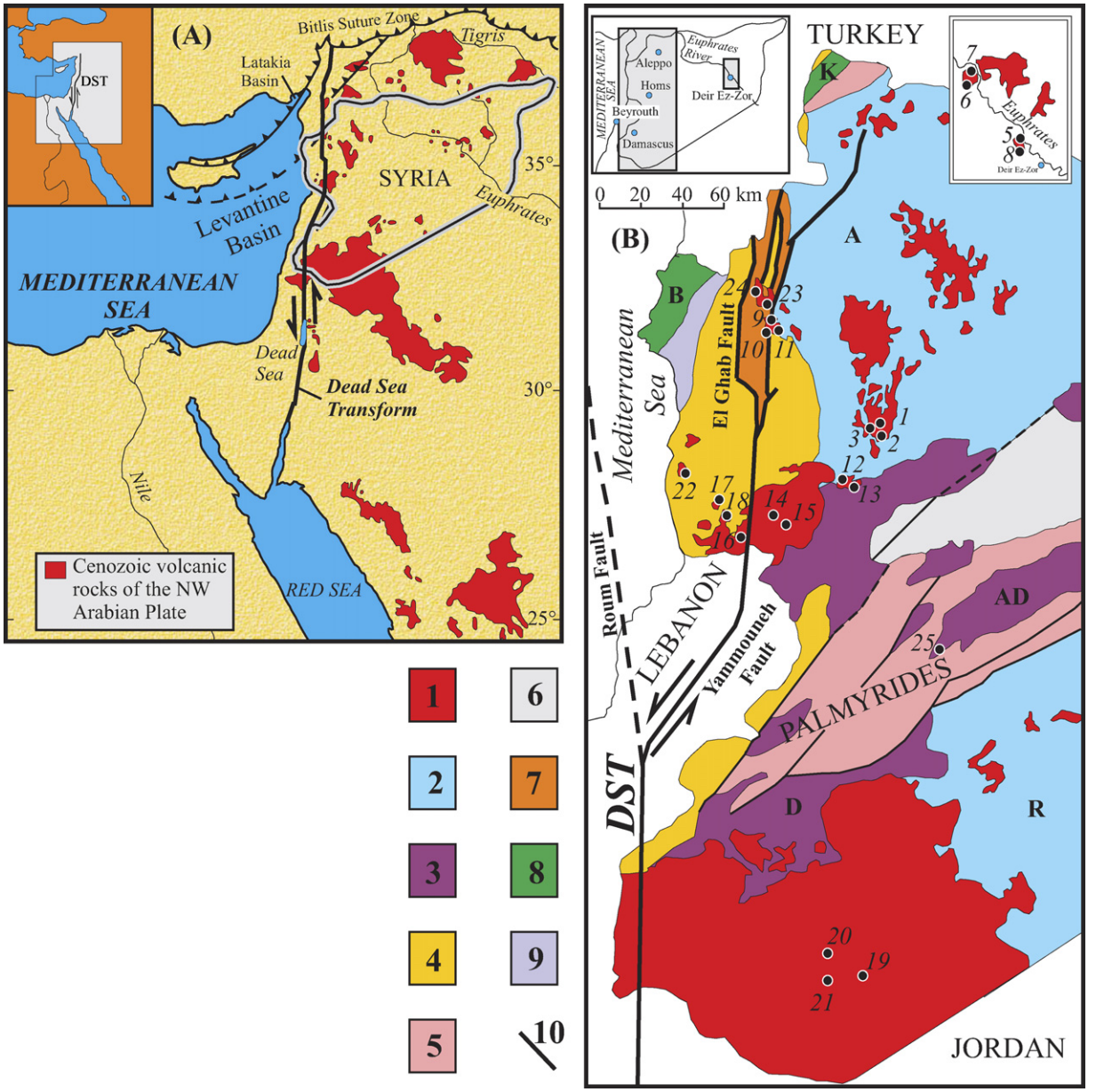

Fig. 1. (A) Main outcrops of Cenozoic volcanic rocks of the Arabian Plate (modified from Garfunkel, 1989). (B) Simplified geological sketch map of Syria (modified from Sharkov et al., 1994, 1998). 1 = late Cenozoic volcanic rocks; 2 = relatively stable platforms (A = Aleppo Platform; R = Rutbah Platform); 3 = molasse basins (D = Damascus Basin; AD = Ad-Daw Basin); 4 = dome-shaped uplifts and horsts; 5 = southern Palmyrides; 6 = northern Palmyrides; 7 = El-Ghab Plio-Quaternary Graben; 8 = platform margins, including Alpine allochnonous masses (B = Bassit-Latakia; K = Kourdag); 9 = Miocene Graben (AK = Al Kebir Graben); 10 = main faults. DST = Dead Sea Transform. Black circles = sample locality (see Table 1).

the Mediterranean coast and the DST from middle Jurassic (~170? Ma) to middle Cretaceous (~148–90 Ma; Mouty et al., 1992; Laws and Wilson, 1997 and references therein).

The Mashrek area (Middle East; SE Turkey, Syria, Lebanon, Jordan, Israel, Palestine and Saudi Arabia) has been the locus of an extensive volcanic activity developed mostly during the last 20 Ma (Fig. 1; Çapan et al., 1987; Giannérini et al., 1988; Garfunkel, 1989; Heimann and Ron, 1993; Mor, 1993; Ilani et al., 2001), post-dating the break-up of Africa and Arabia, opening of the Red Sea and Oligocene flood volcanism in Yemen and Ethiopia (e.g., Baker et al., 1997; Rukieh et al., 2005).

During the Cenozoic, the northward drift of the Arabian plate caused tectonic reorganization, more or less contemporaneous with igneous activity (Giannérini et al., 1988; Zanchi et al., 2002; Rukieh et al., 2005). The main stages are: (a) the development of the DST (also known as the Levantine fault system), a sinistral strike-slip fault with a total length of about 1000 km and a total displacement of about 105 km (e.g., Garfunkel, 1981; LePichon and Gaulier, 1988; Heimann and Ron, 1993; Sobolev et al., 2005; Fig. 1). This fault system accommodated the differential motion between the African plate (moving in a N–NE direction relative to the Eurasian Plate at a rate of ∼10 mm/year) and the Arabian micro-plate (moving in a N–NW direction at a rate of ∼18–25 mm/year; McClusky et al., 2003); (b) the formation of the upper Oligocene–Miocene Palmyrides fold-and-thrust belt, made up of deformed Cretaceous–Paleogene formations, aligned along NE–SW directed anticlinals and synclinals in the western Arabian plate, east of the DST (e.g., Al-Saad et al., 1992; Salel and Seguret, 1994; Litak et al., 1997; Rukieh et al., 2005; Fig. 1) and (c) major Cenozoic (mostly Neogene) volcanic activity (e.g., Mouty et al., 1992; Heimann and Ron, 1993; Sharkov et al., 1998; Bertrand et al., 2003; Shaw et al., 2003; Abdel-Rahman and Nassa, 2004; Fig. 1).

Neogene basaltic magmatism is absent from the deformed zone of the Palmyrides belt, with the exception of the Damascus region, where rare Miocene lavas from the north–westernmost Haurun–Druze plateau are deformed, and from the Ad Daw Basin in central Palmyrides (Giannérini et al., 1988; Sharkov et al., 1994; Rukieh et al., 2005). The Palmyrides belt is a NE–SW oriented chain that can be traced for a total length of about 350 km between the coastal massifs on the left (anti-Lebanon chain) and the Euphrates river on the right (Al-Saad et al., 1992; Fig. 1). This sequence of parallel anticlines separates Syria in two regions (the northern and the southern), both of which have been characterized by volcanic activity during Neogene. The northern sector (the Aleppo Plateau Province, according to the neotectonic map of Rukieh et al., 2005) comprises the Taurus and the Bilas–Bouieda Mts. Volcanic rocks in this sector of Syria outcrop near the coast-line (Aleppo plateau, Shin plateau-Homs area, El Ghab depression and Mt. Saphita; Sharkov et al., 1998) and along the NE continuation of the Palmyrides belt, along the Euphrates river (Deir-ez-Zor locality; NE Syria; the Mesopotamian Basin Province of Rukieh et al., 2005). Rare Paleogene (lower Eocene) tuffs and altered basalts have been observed near the Aafrine Valley (NW from Aleppo; Mouty et al., 1992). South of the Palmyrides, a huge basaltic plateau known as the Harrat Ash Shaam volcanic area (the Jebel Arab Volcanic Province of Rukieh et al., 2005) covers an area larger than 50,000 km^2 (Giannérini et al., 1988; Ilani et al., 2001; Ibrahim et al., 2003; Shaw et al., 2003; Weinstein et al., 2006; Fig. 1). The northernmost sector of this huge plateau rests on Syrian territory and here it assumes the name of Haurun–Druze plateau (Sharkov et al., 1994). The total thickness of lavas reaches 1–1.5 km with dozens of lava flows emanating from several NW–SE oriented vents (Sharkov et al., 1994; Ibrahim et al., 2003). Cinder-pyroclastic cones often contain ultramafic mantle xenoliths (commonly spinel lherzolite, harzburgites, websterites, garnet-pyroxenites and hornblendites; Mittlefehldt, 1984; Sharkov et al., 1996; Nasir and Safarjalani, 2000; Bilal and Touret, 2001). The south–eastern part of Syria (the Rutbah Province of Rukieh et al., 2005) is represented by thick undeformed Phanerozoic sedimentary rocks. Differences in Bouguer gravity values between Aleppo plateau and Rutbah uplift allowed some authors to propose for these regions two different origins as two independent micro-plates amalgamated during late Proterozoic along a suture or a shear zone (now represented by the Palmyrides belt; Best et al., 1990; Litak et al., 1997). According to this view, the Palmyrides belt would have developed in correspondence of an ancient mobile belt, a feature observed also in many other places (e.g., Doglioni, 1995; Vauchez et al., 1997).

During the last few years geochronological and geochemical/petrological studies on the Jordanian and Israeli sectors of the Harrat Ash Shaam have been carried out (e.g., Weinstein, 2000; Ilani et al., 2001; Bertrand et al., 2003; Ibrahim et al., 2003; Shaw et al., 2003; Weinstein et al., 2006) but little attention has been paid on the Syrian volcanic rocks.

3. K/Ar geochronology

During the Miocene, extensive volcanic activity in Syria covers Oligocene and upper Eocene sediments in the Palmyrides and Damascus area (Mouty et al., 1992) and is more or less contemporaneous with, or slightly post-dates the late stages of continent–continent collision between the Arabian and the Eurasian plate (along the Bitlis–Zagros suture zone) and the opening of the Aden-Red Sea rift system (∼26 Ma; Omar and Steckler, 1995). The Arabia–Eurasia collision, characterized by development of nappes and ophiolitic melanges, started in the Maastrichtian with the closure of the Neo-Tethys and continued until lower Miocene (a.o., Litak et al., 1997; Aksu et al., 2005; Rukieh et al., 2005). During upper Oligocene-lower Miocene, the NW propagation of the Aden Sea rift system caused deformation in the

north–westernmost sector of the Arabian plate; the following spreading of Red Sea caused the plate to move to the NE with the final collision along the Zagros line (e.g., Zanchi et al., 2002).

Mouty et al. (1992) proposed a magmatic gap between ~16 and ~8 Ma, but more recent K/Ar investigations show virtually continuous igneous activity in the Syrian sector (Sharkov et al., 1994, 1998). According to Rukieh et al. (2005), a decrease in the volcanic activity is notable during the first phase of neotectonic deformation in Syria (during Burdigalian–Langhian). However, these conclusions are based on the assumption that the K/Ar dates are proportional to the intensity of volcanism. The upper Cenozoic basaltic plateau magmatism of Syria is grouped into three major phases, slightly modifying the scheme proposed by Sharkov et al. (1998): (1) late Oligocene-middle Miocene (?26–16 Ma). K/Ar ages of Syrian basalts evidence that volcanism started ~24–26 Ma ago in the Haurun–Druze plateau but probably it can be dated back to Rupelian (i.e., >28 Ma) in the Palmyrides belt and in the Shin plateau (Mouty et al., 1992; Sharkov et al., 1998); near Aleppo, plateaux lavas are interbedded with Helvetian marine sediments (middle Miocene). The beginning of igneous activity is in concordance with the first stages of spreading of the Red Sea (~30 Ma; Camp and Roobol, 1989). (2) Middle Miocene–Pleistocene (~14–0.8 Ma). During this phase, basaltic magmatism took place both north (Aleppo and Shin Pleateux) and south of the Palmyrides belt (Korazim block, the western sector of the Haurun–Druze plateau and western side of the Jordan River; Heimann and Ron, 1993; Sharkov et al., 1998). A rare occurrence of upper Miocene (~7 Ma) phonolite outcrops near El Kafr (southern Syria; Bilal and Touret, 2001). The few K/Ar data available for the southernmost outcrops of the Aleppo plateau show late Miocene ages (~12–7.8 Ma; Sharkov et al., 1998). Near the Mediterranean Sea coast the small lava fields in the Tartus area (Banias) yield an age of ~4.35 Ma (Sharkov et al., 1998). Early Pliocene–Pleistocene (~5.1–0.8 Ma) basalts are from Haurun–Druze plateau, Korazim block, Jordan River valley, Al Ghab Basin and from the Euphrates River valley. At the northernmost end of the DST, Plio-Pleistocene (~2–0.4 Ma) volcanic activity (alkali basalts to quartz-tholeiites) is recorded in SE Turkey (Çapan et al., 1987). (3) Holocene. The last igneous activity is recorded in SW Syria along the coastal range and in the Haurun–Druze plateau during Quaternary up to historical times (Çapan et al., 1987; Mouty et al., 1992; Sharkov et al., 1998).

The Golan Heights, formely part of Syria but now occupied by Israel, are mostly Plio-Pleistocene (5.2–0.2 Ma) plateaux basalts, up to 1.5 km thick, and cinder cones, whose age roughly decrease from south to north (Heimann and Steinitz, 1988; Garfunkel, 1989; Heimann and Ron, 1993; Mor, 1993; Weinstein et al., 1994, 2006).

4. Analytical techniques

Twenty-five major and trace element whole rock analyses have been carried out at Activation laboratories (Ontario, Canada) according to Code 4Litho package following lithium metaborate/tetraborate fusion ICP and ICP–MS. Loss On Ignition (LOI) measured according standard gravitative methods.

Four Sr and Nd isotopic ratios have been measured at Activation laboratories dissolving samples in a mixture of HF, HNO_3 and $HClO_4$. Rb and Sr were separated using conventional cation-exchange techniques. Sm and Nd were separated by extraction chromatography on HDEHP covered Teflon powder. The analyses were performed on Finnigan MAT 261 8-collector mass-spectrometer in static mode. During the period of work the weighted average of 15 SRM-987 Sr-standard runs yielded 0.710262 ± 11 (2σ) for $^{87}Sr/^{86}Sr$. $^{143}Nd/^{144}Nd$ ratios are relative to the value of 0.511860 for the La Jolla standard. During the period of work the weighted average of 10 La Jolla Nd-standard runs yielded 0.511850 ± 4 (2σ) for $^{143}Nd/^{144}Nd$. Data are corrected for $^{143}Nd/^{144}Nd = 0.511860$. $^{87}Sr/^{86}Sr$ isotopic ratios have been measured on un-leached samples and on samples leached with 6 M HCl at ~150 °C for about 1 h and then repeatedly rinsed with MQ H_2O.

5. Major elements

The samples are mostly high TiO_2 (TiO_2 ~1.8–3.7 wt.%) alkaline mafic rocks with SiO_2 content ranging from ~44.3 to ~52.5 wt.%. On the basis of TAS classification scheme (Le Bas et al., 1986), the upper Cenozoic volcanic rocks of Syria can be classified as alkali basalts and basanites (CIPW normative olivine >10%) plus minor hawaiites and rare tholeiitic basalts (Fig. 2). As a function of MgO content, major elements, recalculated on LOI-free basis and listed in Table 1, show good negative correlation (Al_2O_3 ~11.4–17.6 wt.%), scattered positive correlation (CaO = 8.1–11.0 wt.%; $CaO/Al_2O_3 = 0.48–0.92$) or no correlation (Fe_2O_{3tot} = 10.6–14.6 wt.%, Na_2O = 2.3–4.2 wt.%, K_2O = 0.6–2.2 wt.%, P_2O_5 = 0.3–1.6 wt.%; Fig. 3). Na_2O/K_2O ratios vary from ~1.5 to ~5.6 and show no correlation

Table 1
Major (wt.%) and trace elements (ppm) content as well as Sr–Nd isotopic ratios of Neogene volcanic rocks from Syria. Numbers in the second column indicate the samples in Fig. 1. K/Ar ages from Sharkov et al. (1994, 1998). Total iron expressed as Fe_2O_{3tot}. Mg# calculated assuming $Fe_2O_3/FeO = 0.15$. bdl = below detection limits. Quality control = detection limit wt.% (major elements) and ppm (trace elements). Reference method = 1 (lithium metaborate/tetraborate fusion ICP); 2 (ICP-MS). Cert = certified values; Meas = Measured values. $^{87}Sr/^{86}Sr$ (unl) = unleached sample; $^{87}Sr/^{86}Sr$ (leach) = leached sample

Sample ID	No. in Fig. 1	Locality	Rock Type	Age (K/Ar)	SiO_2	TiO_2	Al_2O_3	Fe_2O_{3t}	MnO	MgO	CaO	Na_2O	K_2O	P_2O_5	L.O.I.	Total	Mg#	Rb	Sr	Ba	Sc	V	Cr	Co	Ni	Y
808	1	Aleppo Plateau	Alkali basalt	10.8	44.56	2.48	13.17	13.02	0.16	7.98	9.58	2.86	1.01	0.58	3.40	98.80	0.58	11	1961	238	18	215	190	48	170	22
809	2	Aleppo Plateau	Alkali basalt	7.8	45.72	2.46	13.67	13.02	0.17	8.39	9.12	3.55	1.24	0.64	1.52	99.49	0.59	18	743	269	18	213	190	47	180	23
808-2	3	Aleppo Plateau	Alkali basalt	12.0	46.36	2.06	14.18	12.39	0.15	6.76	10.04	3.27	0.84	0.41	2.64	99.10	0.55	10	569	318	19	203	200	44	170	20
9237/1	4	Euphrates River valley	Alkali basalt	0.9	44.32	2.62	11.25	12.98	0.16	11.87	9.89	3.26	1.39	0.61	0.84	99.19	0.67	17	748	245	20	240	300	57	310	23
9237/1-A	5	Euphrates River valley	Basanite	1.0	44.11	2.61	11.17	13.17	0.17	11.70	10.25	3.20	1.36	0.62	0.99	99.35	0.67	16	777	244	20	241	340	61	280	21
9239/1	6	Euphrates River valley	Basanite	2.8	43.86	3.28	12.56	13.77	0.17	9.42	10.75	3.26	1.24	0.59	0.61	99.51	0.61	13	794	227	22	282	320	56	220	20
9530/1	7	Euphrates River valley	Basanite	2.9	43.62	3.01	11.87	14.14	0.17	10.57	10.00	2.57	1.09	0.50	1.18	98.72	0.63	11	1010	193	21	264	340	64	280	19
9531/1	8	Euphrates River valley	Alkali basalt	1.5	44.70	2.81	12.14	12.76	0.16	9.57	10.80	3.21	1.53	0.64	1.00	99.33	0.63	16	887	303	22	252	270	49	210	25
9213/1	9	El-Ghab depression	Basanite	2.0	44.21	3.15	14.34	11.97	0.17	7.34	9.72	3.89	2.14	1.07	1.35	99.35	0.58	36	1343	961	17	202	120	26	80	29
9215/1	10	El-Ghab depression	Alkali basalt	1.5	46.58	2.86	16.92	12.88	0.16	4.09	8.14	3.07	0.73	0.47	3.59	99.49	0.42	3	706	387	20	197	120	32	60	23
9212/1	11	El-Ghab depression	Alkali basalt	1.7	46.81	2.52	14.42	12.42	0.17	6.93	9.27	3.64	1.16	0.63	0.58	98.55	0.56	14	763	322	19	201	210	41	90	22
811	12	Shin Plateau (Homs area)	Alkali basalt	12.8	45.54	2.20	13.06	13.03	0.15	7.82	9.64	3.30	0.76	0.48	3.06	99.04	0.57	9	609	197	18	203	250	51	210	19
812	13	Shin Plateau (Homs area)	Basaltic andesite	17.3	50.59	1.75	14.46	10.22	0.14	5.88	9.22	3.18	0.73	0.25	2.65	99.06	0.56	5	408	259	20	209	240	34	130	20
128-3	14	Shin Plateau (Homs area)	Alkali basalt	5.3	43.23	3.48	14.64	12.83	0.17	8.23	8.95	2.17	1.41	0.63	3.40	99.14	0.59	13	1062	360	19	229	130	40	110	25
148-1	15	Shin Plateau (Homs area)	Alkali basalt	4.9	45.15	2.64	14.66	13.20	0.17	8.39	8.97	3.09	1.13	0.69	1.02	99.11	0.59	8	716	269	22	232	220	51	160	27
9208/1	16	Shin Plateau (Homs area)	Hawaiite	5.5	48.34	2.56	15.98	12.16	0.18	4.73	7.88	4.05	1.32	0.50	1.18	98.88	0.47	11	632	215	17	184	30	26	30	28
9206/1	17	Mt. Saphita area	Hawaiite	5.4	46.48	2.90	15.21	13.59	0.18	4.58	9.64	3.62	1.59	0.85	0.77	99.41	0.43	18	724	381	20	222	80	38	50	33
9207/1	18	Mt. Saphita area	Alkali basalt	4.8	46.85	1.94	15.20	12.84	0.16	7.87	9.15	3.07	0.55	0.29	1.31	99.23	0.58	6	474	115	24	216	370	44	120	22
815	19	Haurun-Druze Plateau	Alkali basalt	2.2	46.75	2.75	15.34	12.60	0.17	6.63	10.12	3.69	1.15	0.57	0.07	99.84	0.54	11	654	306	23	246	160	43	100	26
818	20	Haurun-Druze Plateau	Basanite	1.1	45.38	2.51	14.34	12.86	0.17	8.64	8.18	4.17	1.67	0.67	0.01	98.60	0.60	22	765	393	18	180	230	47	190	24
814-2	21	Haurun-Druze Plateau	Hawaiite	1.5	46.83	2.21	15.51	11.66	0.17	8.32	8.16	4.12	1.18	0.49	0.51	99.16	0.62	7	843	287	22	178	160	36	130	24
9205/1	22	Banias area	Alkali basalt	4.4	46.49	2.14	14.64	14.20	0.17	6.97	9.21	2.66	0.70	0.32	1.89	99.40	0.52	7	380	156	26	246	310	54	210	24
805	23	Jisr-Ash-Shaghour Plateau	Basanite	1.3	42.06	3.00	13.39	12.33	0.16	7.73	9.13	3.43	1.25	1.53	5.04	99.05	0.58	15	1539	646	15	181	110	37	110	26
807	24	Jisr-Ash-Shaghour Plateau	Basanite	1.1	44.12	3.09	14.14	13.93	0.17	7.58	8.38	3.91	1.82	0.88	1.17	99.19	0.55	27	992	414	17	190	190	44	160	24
9527/1	25	Palmyrides	Tholeiitic basalt	24.7	47.94	1.85	13.68	11.67	0.14	7.11	8.97	2.71	0.56	0.26	3.99	98.88	0.58	2	434	177	22	204	230	43	200	20
Quality control																										
Detection Limit:					0.01	0.001	0.01	0.01	0.001	0.01	0.01	0.01	0.01	0.01	0.01	0.01		2	2	3	1	5	20	1	20	2
Reference Method:					1	1	1	1	1	1	1	1	1	1	1	1		2	1	1	1	1	2	2	2	1
W-2 Meas					***52.35***	***1.06***	***15.27***	***10.69***	***0.162***	***6.32***	***10.77***	***2.21***	***0.66***	***0.14***				***20***	***188***	***175***	***35***	***263***	***90***	***43***	***80***	***22***
W-2 Cert					52.44	1.06	15.35	10.74	0.163	6.37	10.87	2.14	0.63	0.13				21	190	182	36	262	90	43	70	24
DNC-1 Meas					***47.02***	***0.479***	***18.17***	***9.92***	***0.144***	***10.18***	***11.22***	***1.93***	***0.32***	***0.07***				***4***	***139***	***106***	***31***	***139***	***260***	***53***	***250***	***18***
DNC-1 Cert					47.04	0.48	18.3	9.93	0.149	10.05	11.27	1.87	0.23	0.09				5	145	114	31	148	290	55	250	18
BIR-1 Meas					***47.77***	***0.96***	***15.36***	***11.22***	***0.169***	***9.64***	***13.15***	***1.83***	***0.03***	***0.03***				***bdl***	***105***	***8***	***44***	***322***	***390***	***53***	***180***	***16***
BIR-1 Cert					47.77	0.96	15.35	11.26	0.171	9.68	13.24	1.75	0.03	0.05				0.3	108	7	44	313	380	51	170	16
NIST 1633b Meas					***49.14***	***1.281***	***28***	***11.14***	***0.018***	***0.8***	***2.1***	***0.27***	***2.34***	***0.54***					***1010***	***709***	***40***	***290***				***92***
NIST 1633b Cert					49.24	1.32	28.43		0.02	0.8	2.11	0.27	2.35	0.53					1041	709	41	296				

Table 1 (*Continued*)

Zr	Nb	La	Ce	Pr	Nd	Sm	Eu	Gd	Tb	Dy	Ho	Er	Tm	Yb	Lu	Th	Pb	U	Hf	Ta	Ga	Cu	Zn	$^{87}Sr/^{86}Sr_{(unl.)}$	ε_{Sr}	$^{87}Sr/^{86}Sr_{(leach)}$	ε_{Sr}	$^{143}Nd/^{144}Nd$	ε_{Nd}
121	30	29.5	59.7	7.51	30.9	6.9	2.27	6.1	0.9	4.5	0.8	2.0	0.25	1.4	0.19	1.9	bdl	0.7	3.0	1.9	19	60	120						
156	40	31.5	61.9	7.56	31.2	6.9	2.37	6.3	0.9	4.6	0.8	2.1	0.26	1.4	0.20	3.2	bdl	1.0	3.6	2.7	20	60	130						
123	21	19.7	40.0	5.09	21.4	5	1.77	4.9	0.7	3.8	0.7	1.8	0.24	1.4	0.18	1.6	5	0.6	2.7	1.4	17	70	110						
182	38	35.0	68.7	8.51	35.1	7.8	2.59	6.9	1.0	4.8	0.8	2.1	0.26	1.4	0.17	3.3	bdl	2.1	4.2	2.7	19	60	130						
175	39	35.1	69.4	8.26	33.3	7.3	2.43	6.8	1.0	4.7	0.8	1.9	0.23	1.3	0.18	3.3	bdl	2.3	4.2	2.7	20	60	110						
166	36	31.4	63.2	7.82	32.8	7.2	2.51	6.3	0.9	4.1	0.7	1.8	0.22	1.3	0.17	2.7	bdl	0.9	4.0	2.4	21	80	130						
154	32	27.9	57.4	6.84	27.8	6.2	2.15	5.7	0.8	3.9	0.7	1.7	0.22	1.2	0.16	2.5	bdl	1.0	3.7	2.1	20	90	120	0.70475	4.3	0.70339	-15.0	0.512911	5.3
195	42	37.8	74.2	9.05	36	7.9	2.63	7.6	1.1	5.1	0.8	2.1	0.27	1.5	0.20	3.7	bdl	1.6	4.5	2.9	20	80	90	0.70400	-6.3	0.70353	-13.1	0.512918	5.4
250	70	69.7	125.0	14.40	56.1	11	3.58	9.2	1.3	5.9	1.0	2.5	0.31	1.8	0.22	6.0	6	2.0	4.0	5.4	20	40	60						
168	39	30.0	61.1	7.55	31.2	6.8	2.48	6.2	0.9	4.6	0.8	2.1	0.27	1.6	0.20	2.3	bdl	0.3	3.8	2.7	20	50	80						
144	39	31.3	60.0	7.27	29.7	6.4	2.27	5.9	0.9	4.4	0.8	2.1	0.26	1.5	0.21	2.8	bdl	0.9	3.4	2.5	19	50	100						
110	26	22.8	46.0	5.80	24.3	5.4	1.93	5.2	0.8	3.8	0.7	1.8	0.23	1.3	0.17	1.8	bdl	0.6	2.8	1.7	19	60	120						
104	15	14.3	29.1	3.59	14.8	3.7	1.34	4.1	0.7	3.6	0.6	1.7	0.23	1.4	0.19	1.8	bdl	0.4	2.4	1.0	17	60	50						
213	46	33.0	67.3	8.03	32.5	7.1	2.43	6.9	1.0	4.8	0.8	2.0	0.26	1.5	0.20	2.9	bdl	0.8	4.5	3.4	18	50	60						
176	37	30.2	59.5	7.03	28.2	6.3	2.15	6.2	1.0	4.9	0.9	2.3	0.31	1.9	0.26	2.4	bdl	0.9	3.9	2.2	19	60	80						
199	30	25.8	53.5	6.97	29.8	6.8	2.41	6.7	1.0	5.5	1.0	2.7	0.35	2.1	0.28	1.8	bdl	0.6	4.3	2.0	20	30	100						
209	48	41.2	78.2	9.08	35.6	7.7	2.62	7.8	1.2	6.0	1.0	2.8	0.38	2.2	0.31	3.6	bdl	1.0	4.5	3.0	22	60	110						
126	15	13.6	29.3	3.66	15.7	4	1.46	4.6	0.7	4.1	0.8	2.1	0.28	1.6	0.22	1.2	5	0.4	2.8	0.9	18	50	90						
214	38	30.6	63.8	7.68	31.1	6.7	2.34	6.4	1.0	4.9	0.8	2.2	0.29	1.8	0.26	1.9	bdl	0.5	4.5	2.5	21	60	100						
240	42	38.1	73.9	9.04	36.2	7.4	2.51	6.6	1.0	4.9	0.9	2.4	0.31	1.8	0.23	3.0	10	0.9	5.0	3.2	19	60	120						
218	30	29.3	57.6	7.00	28	6	2.11	5.5	0.8	4.6	0.8	2.2	0.31	1.9	0.25	2.4	bdl	0.8	4.3	2.4	16	40	50						
93	17	15.1	28.9	3.98	17.8	4.7	1.71	5.1	0.8	4.6	0.9	2.4	0.31	1.8	0.24	1.5	bdl	0.3	2.6	1.1	19	70	120						
259	73	65.1	123.0	13.60	51.8	9.5	3.15	8.4	1.1	5.2	0.8	2.0	0.24	1.4	0.18	4.7	bdl	1.4	5.0	4.6	19	40	100						
275	56	41.2	78.3	9.33	37.8	7.8	2.81	7.1	1.0	4.8	0.8	2.0	0.27	1.5	0.18	4.2	14	1.5	5.2	4.7	21	70	150	0.70321	-17.6	0.70326	-16.9	0.512938	5.8
109	16	13.4	28.9	3.63	15.6	4.1	1.47	4.4	0.7	4.0	0.7	1.9	0.26	1.5	0.22	1.5	bdl	0.5	2.7	1.0	18	80	70	0.70485	5.7	0.70386	-8.4	0.512842	3.9
4	1	0.1	0.1	0.05	0.1	0.1	0.05	0.1	0.1	0.1	0.1	0.1	0.05	0.1	0.04	0.1	5	0.1	0.2	0.1	1	10	30						
1	2	2	2	2	2	2	2	2	2	2	2	2	2	2	2	2	2	2	2	2	2	2	2						
82	*7*	*11*	*23.2*	*2.97*	*12.6*	*3.2*	*1.15*	*3.8*	*0.7*	*4*	*0.8*	*2.4*	*0.34*	*2.1*	*0.31*	*2.2*	*8*	*0.5*	*2.4*	*0.5*	*18*	*110*	*80*						
94	8	10	23	5.9	13	3.3	1		0.6	3.6	0.8	2.5	0.38	2.1	0.33	2.4	9	0.5	2.6	0.5	17	110	80						
33	*1*	*3.6*	*7.7*	*1.01*	*4.5*	*1.3*	*0.59*	*1.9*	*0.4*	*2.6*	*0.6*	*1.9*	*0.28*	*1.9*	*0.28*	*0.2*	*bdl*	*bdl*	*0.9*	*bdl*	*13*	*90*	*60*						
41	3	3.8	11	1.3	4.9	1.4	0.59	2	0.4	2.7	0.6	2	0.38	2	0.32	0.2	6	0.1	1	0.1	15	100	70						
14	*bdl*	*0.8*	*1.9*	*0.39*	*2.3*	*1.1*	*0.54*	*1.9*	*0.4*	*2.6*	*0.6*	*1.8*	*0.26*	*1.7*	*0.25*	*bdl*	*bdl*	*bdl*	*0.5*	*bdl*	*16*	*120*	*70*						
16	0.6	0.6	2	0.38	2.5	1.1	0.54	1.9	0.4	2.5	0.6	1.7	0.26	1.6	0.26	0.03	3	0.01	0.6	0.04	16	130	70						
220																													

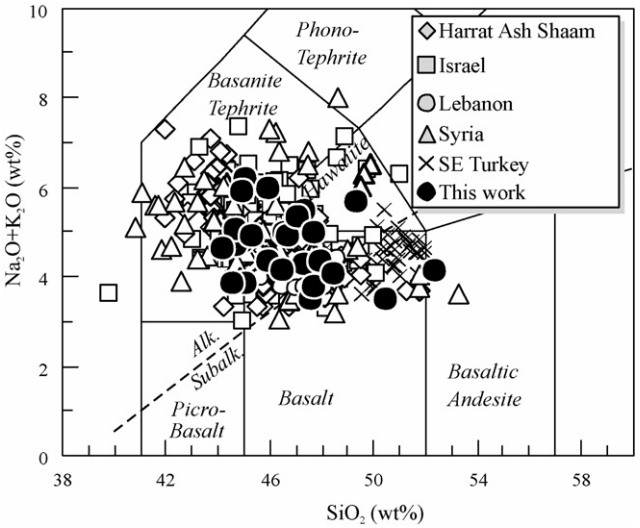

Fig. 2. Total alkali vs. silica classification diagram (Le Bas et al., 1986). All the analyses have been recalculated to LOI-free basis. Dashed line: alkaline–subalkaline division according to Irvine and Baragar (1971). References: SE Turkey (Çapan et al., 1987); Harrat Hash Shaam (Barberi et al., 1979; Altherr et al., 1990; Ibrahim et al., 2003; Shaw et al., 2003); Israel (Stein and Hofmann, 1992; Weinstein, 2000; Weinstein et al., 1994, 2006); Lebanon (Abdel-Fattah et al., 2004); Syria (Mouty et al., 1992; Sharkov et al., 1994, 1996; Fediuk and Al Fugha, 1999).

with MgO content but good positive correlation with SiO_2 (not shown). Mg# values range from composition in equilibrium with peridotitic assemblage (0.67 at MgO = 12.1 wt.%) to more evolved compositions (0.42 at MgO = 4.3 wt.%). LOI is mostly <2 wt.%; only few samples reach higher values up to 5 wt.%.

The analyzed samples fall well within the field described by other Neogene volcanic rocks from Mashrek (Fig. 2), in particular those from the northernmost segment of the DST in SE Turkey (Çapan et al., 1987; Polat et al., 1997; Alici et al., 2001), the Jordanian sector of the Harrath Ash Shaam plateau (Barberi et al., 1979; Altherr et al., 1990; Ibrahim et al., 2003; Shaw et al., 2003), Israel (Golan Heights and Galilee; Weinstein, 2000; Stein and Hofmann, 1992; Weinstein et al., 1994, 2006), north Lebanon (Akkar Province; Abdel-Rahman and Nassa, 2004) and other Syrian volcanic rocks (Mouty et al., 1992; Sharkov et al., 1994, 1996; Fediuk and Al Fugha, 1999).

6. Trace elements

Selected trace elements (Table 1) have been plotted against MgO in Fig. 4. Large Ion Lithophile (LIL) elements like Rb (2–36 ppm), Sr (380–1961 ppm) and Ba (115–961 ppm) show no correlation with MgO and fully lie in the field defined by the other Neogene volcanic rocks of Mashrek (Fig. 4). With respect to SiO_2, LIL elements show variable but negative correlation (especially for Sr; not shown). The highest LIL element concentration (e.g., Sr > 1000 ppm; Rb > 25 ppm; Ba > 400 ppm) are probably the effect of post-magmatic alteration.

Transition elements, such as Sc (15–26 ppm) show no correlation with MgO content (similarly to the other volcanic rocks of Mashrek), whereas Cr (30–370 ppm), Co (26–64 ppm) and Ni (30–310 ppm) show positive correlation (Fig. 4). No substantial differences can be seen between Syrian samples and the other Cenozoic volcanic rocks of Mashrek in terms of transition elements content. An exception is V (184–282 ppm) that shows rough positive correlation with MgO content, opposite to what seen for Mashrek volcanic rocks.

High Field Strength (HFS) elements like Zr (93–275 ppm), Nb (15–73 ppm), Hf (2.4–5.2 ppm), Ta (0.9–5.4 ppm) and Y (19–33 ppm) fall within the field of the other Cenozoic volcanic rocks of Mashrek and show no correlation with MgO. The same elements (with the exception of Y) show negative correlation with SiO_2, a feature also observed for "anorogenic" Plio-Quaternary volcanic rocks of Sardinia (Italy; Lustrino et al., 2002, in press). Other strongly incompatible elements like U, Pb, Th, show the same behaviour of HFS elements (i.e., no correlation with MgO and negative correlation with SiO_2).

REE are variably fractionated with La ranging from ~60 to ~300 times chondrite CI (mostly comprised between 100 and 200 times) and HREE clustering at lower values (Lu ~7–11 times chondrite; Fig. 5); $(La/Lu)_N$ ratio ranges

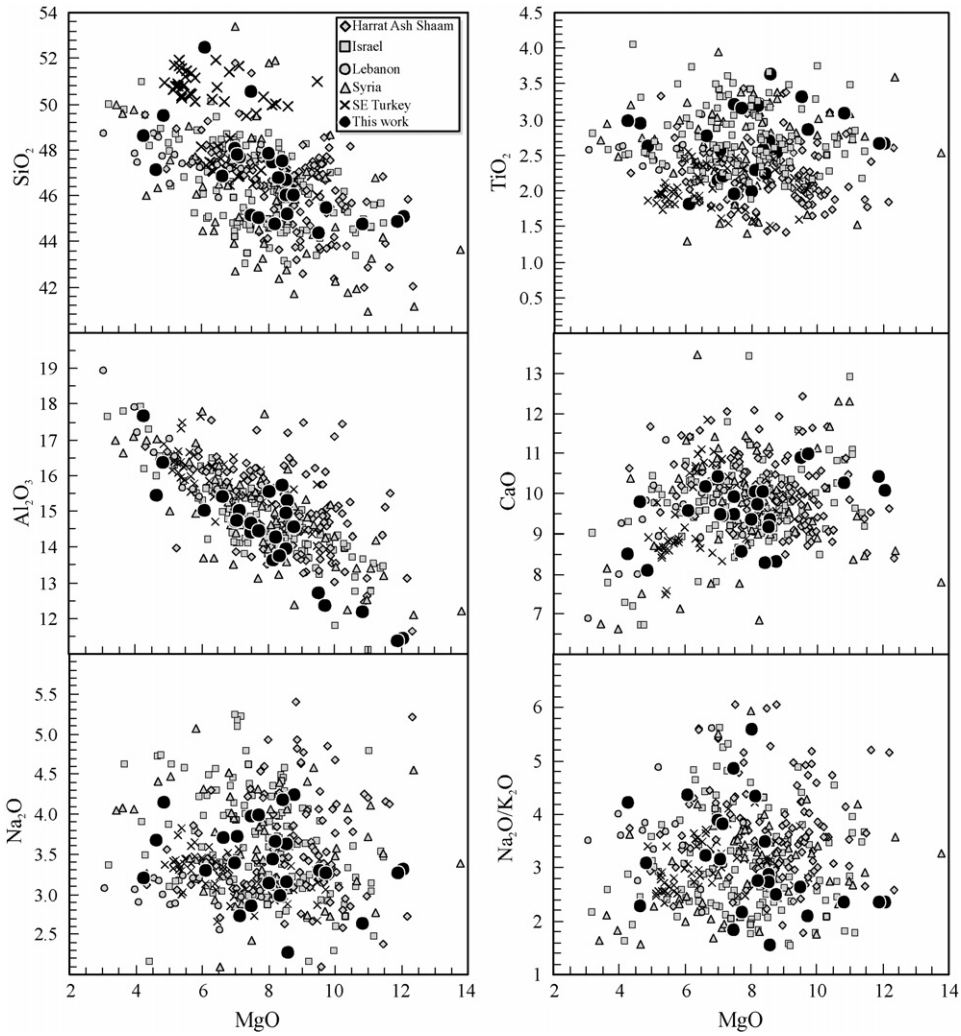

Fig. 3. Selected major elements vs. MgO diagrams. All the analyses have been recalculated to LOI-free basis. References as in Fig. 2.

from ~6 to ~38. Eu/Eu* ratios are slightly above 1 (1.03–1.15) and show no correlation with MgO or with other differentiation indexes (e.g., SiO_2 and Zr content). Middle Rare Earth Elements (MREE)/Heavy REE (HREE) ratios decrease with increasing SiO_2 (e.g., Gd/Yb ratio varies from 6.0 at SiO_2 = 44.74 to 2.9 at SiO_2 = 52.97 wt.%; Fig. 6) but show only slightly positive correlation with MgO (not shown). Total overlap between the Cenozoic Mashrek volcanic rocks (Shaw et al., 2003; Weinstein et al., 2006) and the Syrian samples is evident in Fig. 5.

Incompatible-incompatible trace element diagrams show general positive correlation (e.g., LILE versus Zr, HFSE versus Zr and LREE versus Zr; Fig. 7) even if with some scatter. Zr has been chosen as differentiation index because of its strongly incompatible behaviour in basaltic liquids and because it is easily analyzed by XRF, ICP–MS and INAA. Notwithstanding Zr and La abundances of the Syrian samples analyzed in this study fall well within the field of the other volcanic rocks of Mashrek, La versus Zr diagram evidences that the Syrian samples are offset from the general trend of the Mashrek lavas, being displaced toward higher La (and other LREE) for a given Zr. With regard to transition elements, Sc is the only one showing rough negative correlation with Zr, whereas V, Cr and Ni show major scattering; Y shows rough positive correlation with Zr. Key incompatible trace element ratios (e.g., Ba/Nb, Ba/La, La/Nb, Th/Ta) remain virtually unchanged with decreasing Zr (Fig. 7).

Primitive Mantle (PM)-normalized multi-elemental diagrams for the most mafic samples (MgO > 7 wt.%) from Syria and neighbouring areas (Lebanon, Jordan, Israel) are shown in Fig. 8. The analyzed mafic rocks display typical

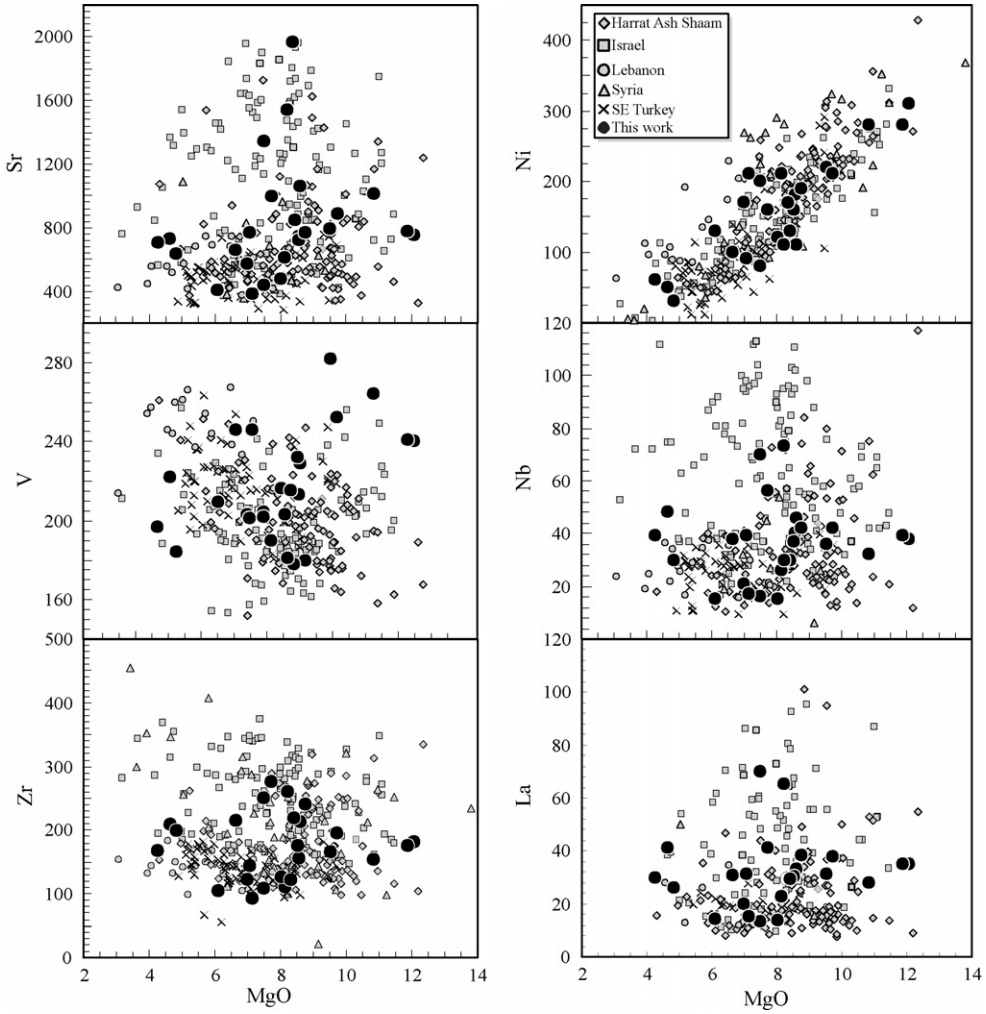

Fig. 4. Selected trace elements vs. MgO diagrams. References as in Fig. 2.

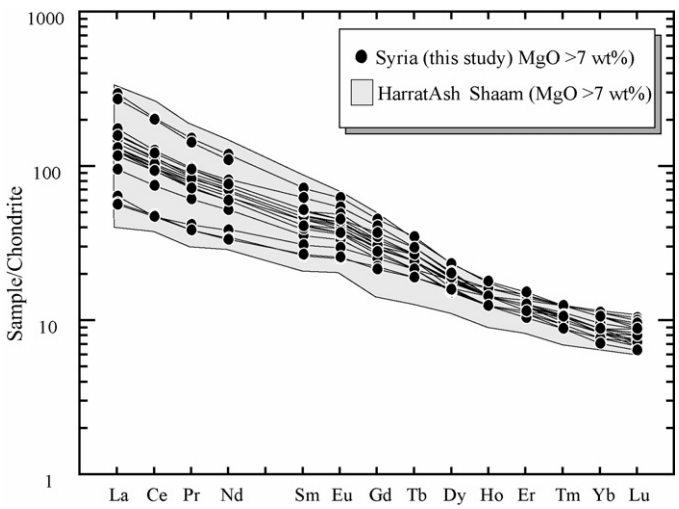

Fig. 5. Chondrite-normalized REE diagram (normalization factor from Sun and McDonough, 1989) for the most primitive (MgO > 7 wt.%) lavas from Syria and Harrat Ash Shaam.

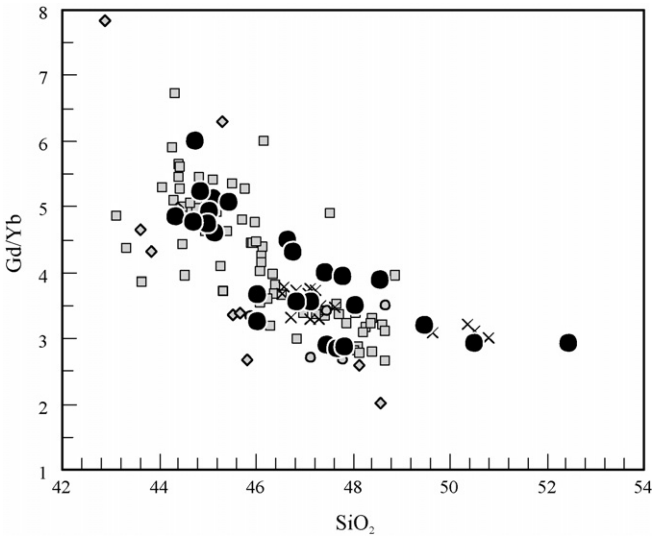

Fig. 6. Gd/Yb vs. SiO_2 diagram. References as in Fig. 2. Gd/Yb ratio reflects MREE/HREE ratio.

within-plate geochemical signatures, with Nb–Ta positive peaks (∼40–150 times PM estimates), K through (∼20–70 times PM) and overall bell-shaped pattern, resembling that of the less differentiated (MgO > 5 wt.%) St. Helena Island rocks in South Atlantic (considered to be the typical HIMU-OIB; Kogarko et al., 1984; Newsom et al., 1986; Weaver et al., 1987; Chaffey et al., 1989; Thirlwall, 1997; Willbold and Stracke, 2006). The only differences rest on the positive Pb anomalies (∼70–200 times PM) seen in the Syrian samples absent in St. Helena basalts, and in the slightly higher Sr (∼20–100 times PM) and P (∼10–70 times PM) contents of the former. With regard to Pb anomalies it is to note that they are possibly related to analytical difficulties in analyzing this element at low concentration. Anomalously low Ce/Pb ratios (4 out 5 samples have Ce/Pb <8, compared to ∼25 for oceanic basalts; Hofmann et al., 1988; Miller et al., 1994) of Syrian lavas, coupled with "normal" Nb/U values (average Nb/U ∼43 for 20 out 25 samples, compared to values of ∼45 for oceanic basalts) can be therefore interpreted as artificial Pb excess caused by analytical techniques rather than true expression of anomalous mantle sources.

Peaks in correspondence of Ba is a typical feature of Syrian samples and in general of the volcanic rocks from Mashrek area (Fig. 8). With few exceptions, $(Ba/Nb)_N$ and $(La/Nb)_N$ ratios are always <1. As a whole, the mafic volcanic rocks of Mashrek indicate a relatively coherent homogeneous composition, with the exception of some negative Pb anomalies seen for some Harrat Ash Shaam volcanic rocks (mostly from the Jordanian and Israeli sectors; Shaw et al., 2003; Weinstein et al., 2006).

7. Sr–Nd isotopes

Four representative samples analyzed for Sr–Nd isotopic systematics are listed in Table 1 and plotted in Fig. 9. With one exception, $^{87}Sr/^{86}Sr$ isotopic ratios measured on un-leached samples show constantly higher values (0.70321–0.70485) compared to $^{87}Sr/^{86}Sr$ ratios of samples leached with HCl (0.70326–0.70386). No recalculation to initial values was done because of the young age of the samples and/or the very low $^{87}Rb/^{87}Sr$ ratios. $^{87}Sr/^{86}Sr$ isotopic ratios of Syrian lavas show good negative correlation with $^{143}Nd/^{144}Nd$ ratios (ranging from 0.512938 to 0.512842), similarly to what observed for Jordanian basalts (e.g., Shaw et al., 2003). In this case Shaw et al. (2003) related this correlation to contamination with upper crustal lithologies. In contrast with the trend observed for Syrian and Jordanian lavas, the Golan–Galilee (Israel) basalts show variable $^{87}Sr/^{86}Sr$ isotopic ratios (0.70312–0.70337) with nearly uniform $^{143}Nd/^{144}Nd$ (0.51285–0.51291; Weinstein et al., 2006). The leached samples show Sr–Nd isotopic ratios overlapping those of the rest of the Cenozoic volcanic rocks from Mashrek (ranging from 0.51297 to 0.51262; Çapan et al., 1987; Altherr et al., 1990; Weinstein, 2000; Bertrand et al., 2003; Shaw et al., 2003; Weinstein et al., 2006). Among Mashrek lavas, those from Israel are characterized by lower $^{87}Sr/^{86}Sr$ for a given $^{143}Nd/^{144}Nd$ (Stein and Hofmann, 1992) compared to the Syrian and the Harrat Ash Shaam products.

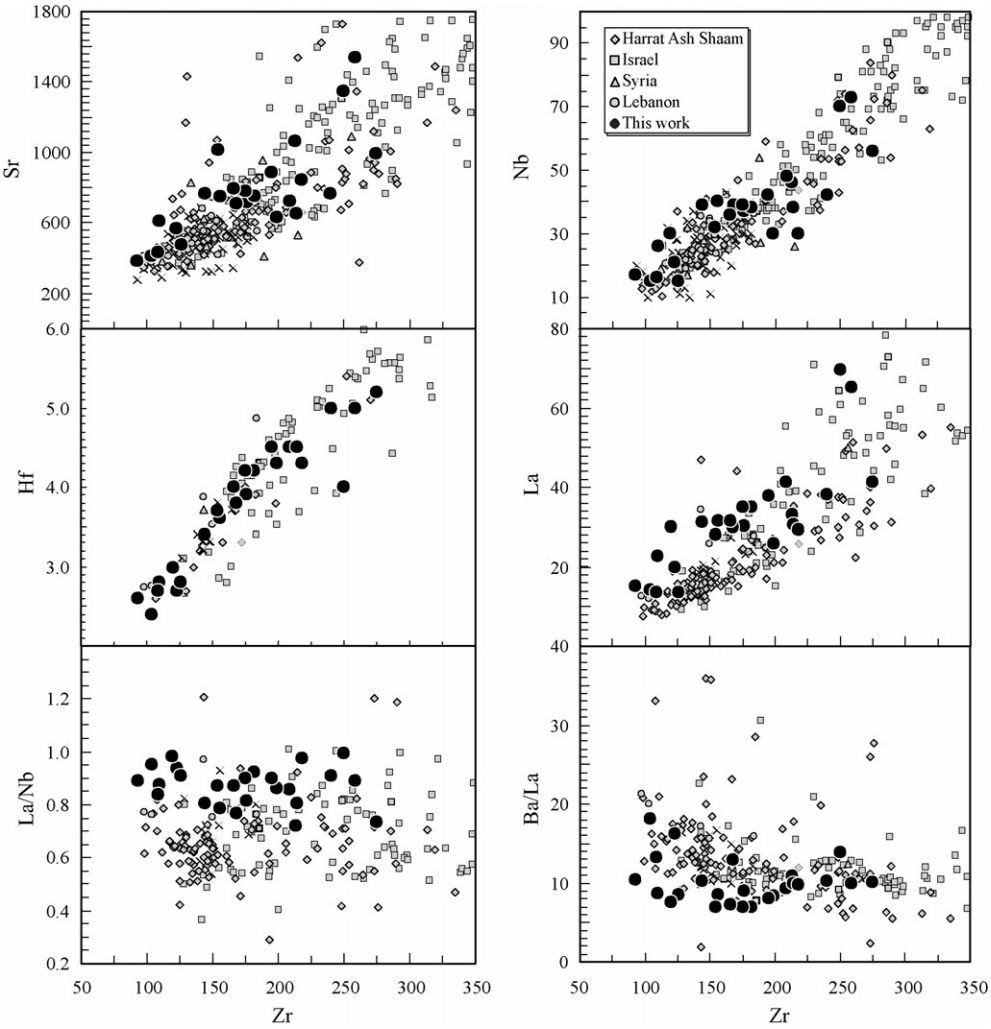

Fig. 7. Selected trace elements vs. Zr diagrams. References as in Fig. 2.

8. Discussion

8.1. Fractional crystallization

The Syrian samples analyzed in this study range from relatively primitive (Mg# ~0.67) to evolved compositions (Mg# ~0.42), implying a role for fractional crystallization of high Mg# phases. This kind of process is hard to model quantitatively because of an absence of clear correlations between major elements and the decoupled behaviour between incompatible and compatible trace elements and major elements. Fractional crystallization of mildly alkaline basaltic magmas with high MgO and Mg# involves almost essentially olivine and clinopyroxene removal, followed, later on, by Fe–Ti oxides and plagioclase (by comparison, MORB liquids have generally plagioclase and olivine on the liquidus). Olivine ($Fo_{81\text{-}72}$; Sharkov et al., 1996) is the most abundant phenocrysts of Syrian rocks, followed by clinopyroxene ($Wo_{47\text{-}51}En_{40\text{-}32}Fs_{17\text{-}13}$; Sharkov et al., 1996) and, in minor amount, by plagioclase. The groundmass is made up of microcrystalline plagioclase ± cpx ± olivine ± Fe–Ti oxides. These petrographic features are typical also of Lebanese (Abdel-Rahman and Nassa, 2004), Jordanian (Shaw et al., 2003) and Israeli (Weinstein, 2000; Weinstein et al., 2006) Cenozoic volcanic rocks. Therefore, petrography indicates that the most important crystallizing phases are olivine and clinopyroxene followed, only in rare cases (and in small amount) by plagioclase (plagioclase phenocrysts content generally is <1%). In summary, olivine and clinopyroxene, but not plagioclase participate to fractional crystallization

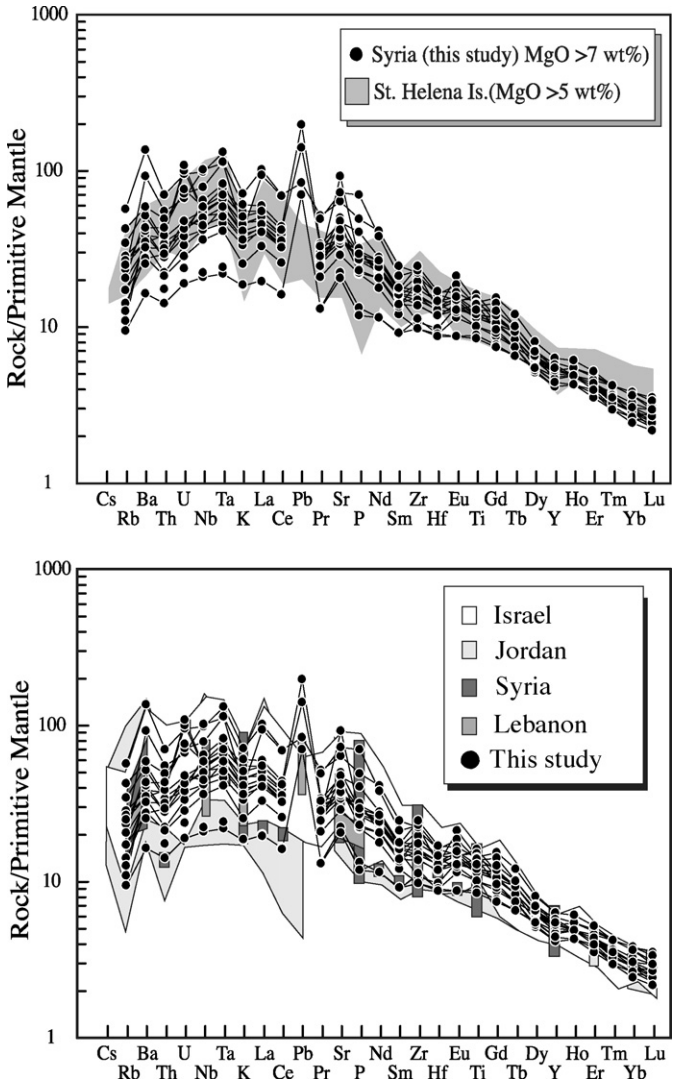

Fig. 8. Multi-elemental primitive mantle-normalized diagram (normalization factors from McDonough and Sun, 1989) for the most primitive (MgO > 7 wt.%) lavas from Syria and neighbouring areas. Reference as in Fig. 2. The field of St. Helena basalts (Kogarko et al., 1984; Newsom et al., 1986; Weaver et al., 1987; Chaffey et al., 1989; Thirlwall, 1997; Willbold and Stracke, 2006) has been plotted for comparison. Pb positive anomalies of Syrian basalts are probably caused by analytical techniques rather than true expression of anomalous mantle sources (see text for more details).

processes; petrography, Al_2O_3, CaO/Al_2O_3, Sr, Sc and Ni content and variation are consistent with this, in agreement also with the conclusions of Weinstein et al. (2006) carried out on Plio-Pleisteocene volcanic rocks of Israel.

Most correlations of major and trace elements vs. strongly incompatible elements (e.g., Zr) are poor (e.g., Fig. 7) because of the possible existence of more than one liquid line of descent, alteration effects or phenocrysts accumulation. This means that whole rock composition may be in part different from the original melt composition.

8.2. *Upper crustal contamination*

Significant upper crustal contamination is considered unlikely on the basis of several arguments. The most mafic alkaline rocks from Syria contain often mantle xenoliths up to 30 cm in diameter (e.g., Sharkov et al., 1996; Nasir and Safarjalani, 2000; Bilal and Touret, 2001), and this implies rapid ascent of the host magma to the surface, with limited possibility of interaction with crustal lithologies (e.g., Spera, 1984; Lustrino et al., in press). Upper crustal contamination would lead to a modification of canonical trace element ratios (especially HFSE/LILE ratios) that, on

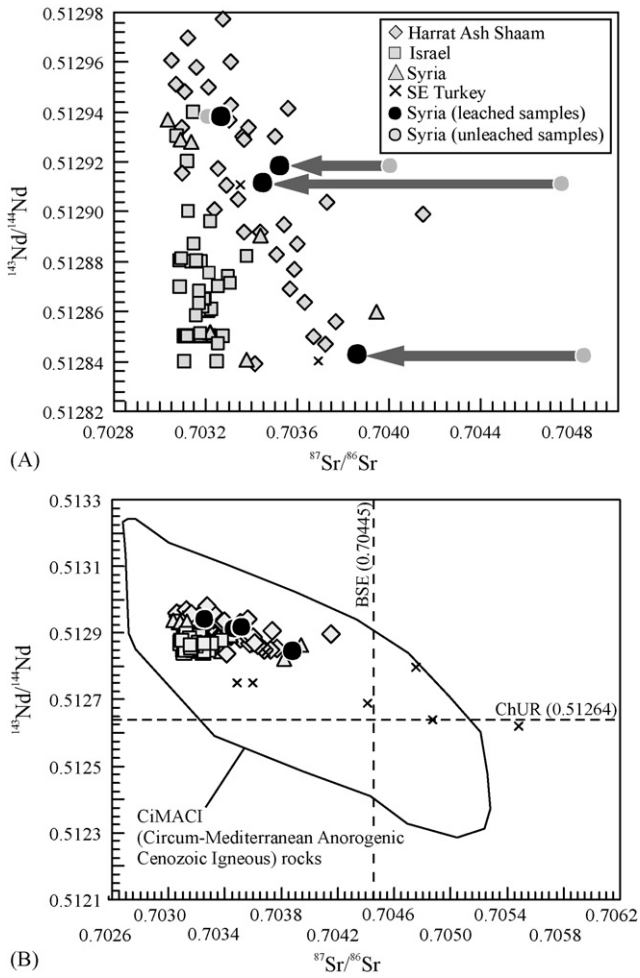

Fig. 9. (A) $^{143}Nd/^{144}Nd$ vs. $^{87}Sr/^{86}Sr$ isotopic ratios for Syrian lavas and neighbouring areas. Grey arrows represent correction to the $^{87}Sr/^{86}Sr$ ratios. Grey circles represent $^{87}Sr/^{86}Sr$ isotopic composition of un-leached Syrian samples; black circles represent leached samples. Symbols and references as in Fig. 2. (B) $^{143}Nd/^{144}Nd$ vs. $^{87}Sr/^{86}Sr$ isotopic ratios for Syrian lavas compared to the rest of the CiMACI (Circum-Mediterranean Cenozoic Igneous) Province (Lustrino and Wilson, in press). ChUR = Chondrite Uniform Reservoir. BSE = Bulk Silicate Earth.

the other hand, remain roughly uniform in the Syrian volcanic rocks. Moreover, also Nb–Ta peaks are inconsistent with upper crustal contamination. What is, then, the cause of Sr–Nd isotopic variability? One possibility is the presence of limited upper crustal contamination (i.e., few percent) with ancient (i.e., Proterozoic) basement with extremely radiogenic Sr and unradiogenic Nd isotopic compositions, as that present in the Arabian shield (e.g., Hegner and Pallister, 1989). Another possibility is the presence of upper mantle sources that are heterogeneous in terms of Sr–Nd isotopic ratios and less heterogeneous in terms of incompatible trace elements. This last option was considered by Shaw et al. (2003) to explain the relative large Sr–Nd isotopic variation of Jordanian sector of the Harrat Ash Shaam volcanic rocks. According to these authors, the major and trace element variation and the Sr–Nd–Pb isotopic range of the Jordanian lavas cannot be explained by fractional crystallization and crustal contamination alone, but requires polybaric melting of heterogeneous mantle sources.

8.3. Origin of Sr–Nd radiogenic variability

With one single exception, $^{87}Sr/^{86}Sr$ values of volcanic rocks from Harrat Ash Shaam plateau are <0.70377 (Fig. 9; Altherr et al., 1990; Weinstein, 2000; Bertrand et al., 2003; Shaw et al., 2003; Weinstein et al., 2006), enveloping the $^{87}Sr/^{86}Sr$ values of Syrian lavas. Bertrand et al. (2003) reported some relatively radiogenic Sr compositions

($^{87}Sr/^{86}Sr = 0.70382–0.70394$) for two outcrops NE of Djebel Druze plateau (the Harrat Ash Shaam plateau outcropping in the Syrian territory) and related them to source heterogeneity rather than crustal contamination or alteration effect. The relatively radiogenic Sr and unradiogenic Nd isotopic composition of lavas emplaced along the northernmost sector of the DST in SE Turkey (Hassa Graben and Karasu Valley; Fig. 9) are measured in quartz tholeiites whose origin is considered to reflect variable degrees of interaction of mantle-derived melts with crustal lithologies (Çapan et al., 1987; Alici et al., 2001). Shaw et al. (2003) noted that the effect of alteration [as exemplified by iddingsitic rims of olivine and secondary growth of carbonate material (*caliche*) being distributed in cavities throughout the rock] can increase the Sr isotopic ratios, leaving virtually unchanged Nd isotopes. On the other hand, Weinstein et al. (2006) concluded that the degree of crustal contamination of all the Phanerozoic basalts from Israel is probably small on the basis of their Sr and Nd isotopic composition.

8.4. What did happen in lower Pliocene?

Taken as a whole, major and trace element content of Cenozoic Mashrek volcanic rocks seem not correlated with age. However, the few Syrian samples older than 15 Ma for which K/Ar age determination and complete geochemical data do exist (e.g., sample 9527/1 from Palmyrides and sample 812 from Aleppo plateau) are characterized by relatively low incompatible trace elements content. Younger lavas (i.e., <15 Ma old) show a large range of incompatible trace element content (Fig. 10).

Based on major elements (TiO_2, Na_2O, K_2O and P_2O_5) and many incompatible trace elements (in particular, Rb, Sr, Ba, Zr, Nb, REE, Th, U, Hf and Ta) content, the Syrian lavas can be divided into two groups (Fig. 10). The first group comprises lavas emplaced between ~25 and ~5 Ma, whereas the second group comprises lavas emplaced between ~5 and ~1 Ma. Both groups show the same variation with age, i.e., increasing content of incompatible elements with decreasing age. At ~5 Ma, a major break is seen as consequence of an abrupt change of major and incompatible trace element content.

What can be the cause of the abrupt change of magma composition at ~5 Ma? Two possibilities have been investigated: (1) upper crustal contamination of basaltic magma and (2) arrival of a new batch of mantle-derived magma with different composition.

As a general rule, upper crustal contamination of basaltic melts leads to increase in SiO_2 and alkalies and a decrease in MgO and TiO_2 in hybrid melts. The content of other oxides like Al_2O_3, Fe_2O_3 or CaO depends on the composition of the starting basaltic melt and the crustal contaminant. At the Miocene–Pliocene boundary, the basaltic rocks from Syria show an abrupt decrease in TiO_2, Na_2O, K_2O and P_2O_5 but not an increase in SiO_2 or a decrease in MgO, as it would be expected in an upper crust contamination process. Moreover, upper crust contamination would lead to Rb and Ba increase, opposite to what seen for the oldest Syrian rocks of the second cycle. Significant upper crustal contamination as the cause of the break in composition at ~5 Ma can be considered unlikely also because of the absence of a drop in transition elements content like Cr, V, Sc and Ni. Lastly, important canonical rations like Nb/U, Rb/Sr, Ce/Pb, Ba/Nb, La/Nb and Ba/La remain virtually unchanged at the ~5 Ma threshold, thus reinforcing the hypothesis that upper crustal contamination cannot be the cause of the abrupt major and trace element content variation of the Syrian lavas at ~5 Ma.

The second possibility considers the possibility that a new thermo-baric regime develops at the Miocene–Pliocene boundary. According to this hypothesis, during the ~25–5 Ma time interval, the degree of partial melting of the upper mantle is more or less constant and different batches of magma undergo variable degrees of fractional crystallization. This activity is considered to be related to occasional trans-tensional movements along the DST, therefore caused by passive upwelling of upper mantle. At ~5 Ma, a larger degree of partial melting (or a shallower depth of partial melting) would generate liquids with different contents of incompatible trace elements but with similar ratios. This new batch of magma would have lower incompatible trace element content and lower TiO_2, Na_2O, K_2O and P_2O_5 abundances, as consequence of the dilution effects of relatively larger degrees of melting. This type of basaltic magma could have been produced by moderate to relatively high degrees of partial melting, or by partial melting of shallower (but geochemically similar) mantle sources, coherently with their mildly alkaline, transitional to tholeiitic whole rock composition. Substantial changes in mantle sources is considered unlikely because of the absence of variation of canonical ratios between the two volcanic cycles. The relative constancy of strongly incompatible elements ratios speak for a potentially similar source that has melted either at higher degrees or at shallower depths. The wide concentration

range of incompatible elements in the Golan–Galilee (Israel) basalts was related by Weinstein et al. (2006) to mantle source heterogeneity or to variable degree partial melting.

A recent high-resolution multi-channel seismic reflection study carried out by Hall et al. (2005) provides clues for the geochemical change of Syrian lavas at the Miocene–Pliocene boundary. Hall et al. (2005) show that the Cenozoic evolution of the Latakia Basin (easternmost Mediterranean Sea along the north-westernmost sector of Syria; Fig. 1) can be described in two distinct tectonic phases. The first phase was characterized by SE-directed contraction and lasted until the latest Miocene; the second phase started in the lower Pliocene and was characterized by extension related to the initiation of strike-slip movements along the eastern Anatolian Transform Fault. The data of Hall et al. (2005) evidence, thus, a net change in kinematic regime during the lower Pliocene, with the end of SE-directed thrusting and start of trans-tension with the development of horst and graben structures, bounded by faults linked on-land with the East Anatolian Transform Fault. A detailed paleostress structural study carried out on NW Syria outcrops by Zanchi et al. (2002) reached similar conclusions, showing that carbonate successions of late Cretaceous and late Miocene (Tortonian) age in the Aleppo plateau show gentle folding, whereas Pliocene sediments are generally undeformed.

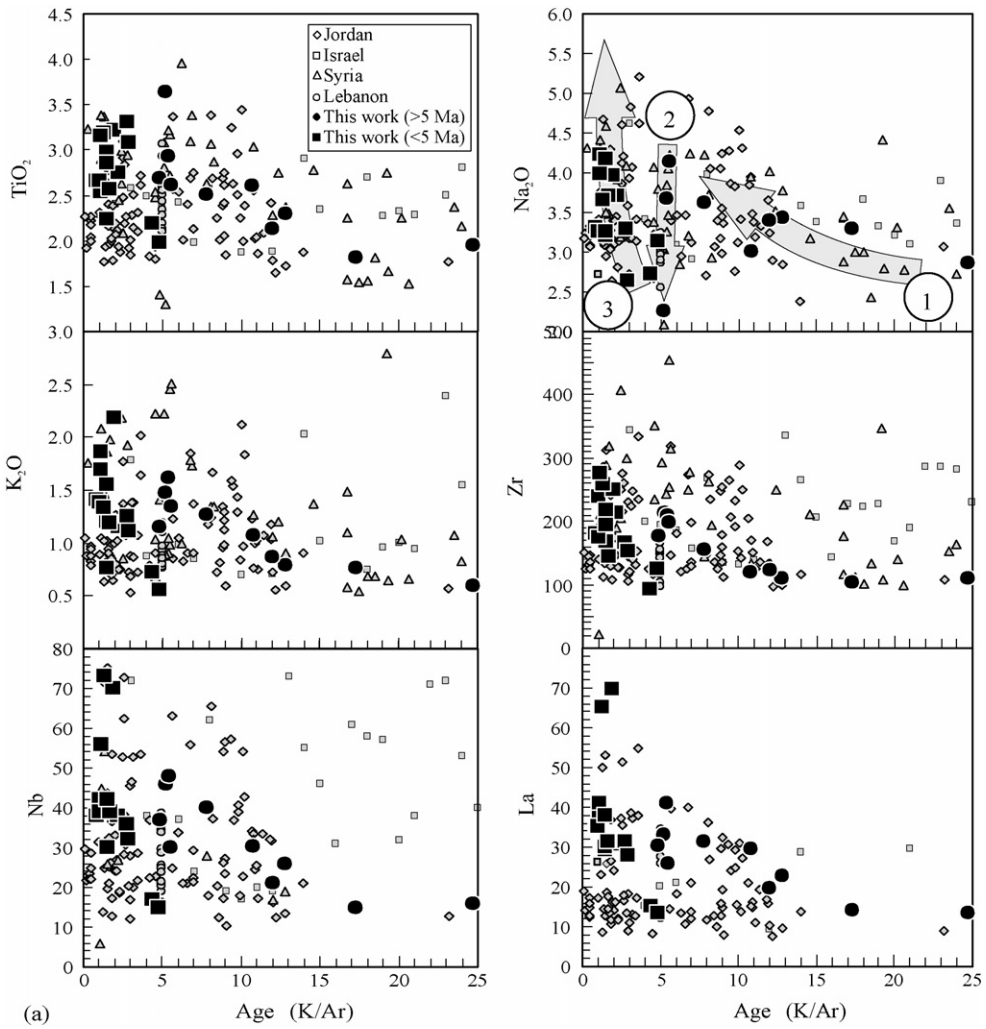

Fig. 10. (a, b) Key major and trace elements vs. age diagrams. Black circles = Syrian samples older than ~5 Ma. Black squares = Syrian samples younger than ~5 Ma. Other symbols as in Fig. 2. Arrow 1 = Vector indicating qualitative effects of fractional crystallization. Arrow 2 = Vector indicating qualitative effects of increasing degree of partial melting in relatively short time. Arrow 3 = Vector indicating qualitative effects of fractional crystallization. The overall pattern shown in these two figures can be interpreted as a consequence of a major variation in thermo-baric conditions in a relatively short time interval at the Miocene–Pliocene boundary (~5 Ma). The evolution of basaltic melts before and after this date is mostly controlled by fractionation of olivine + clinopyroxene assemblage (see text for more details).

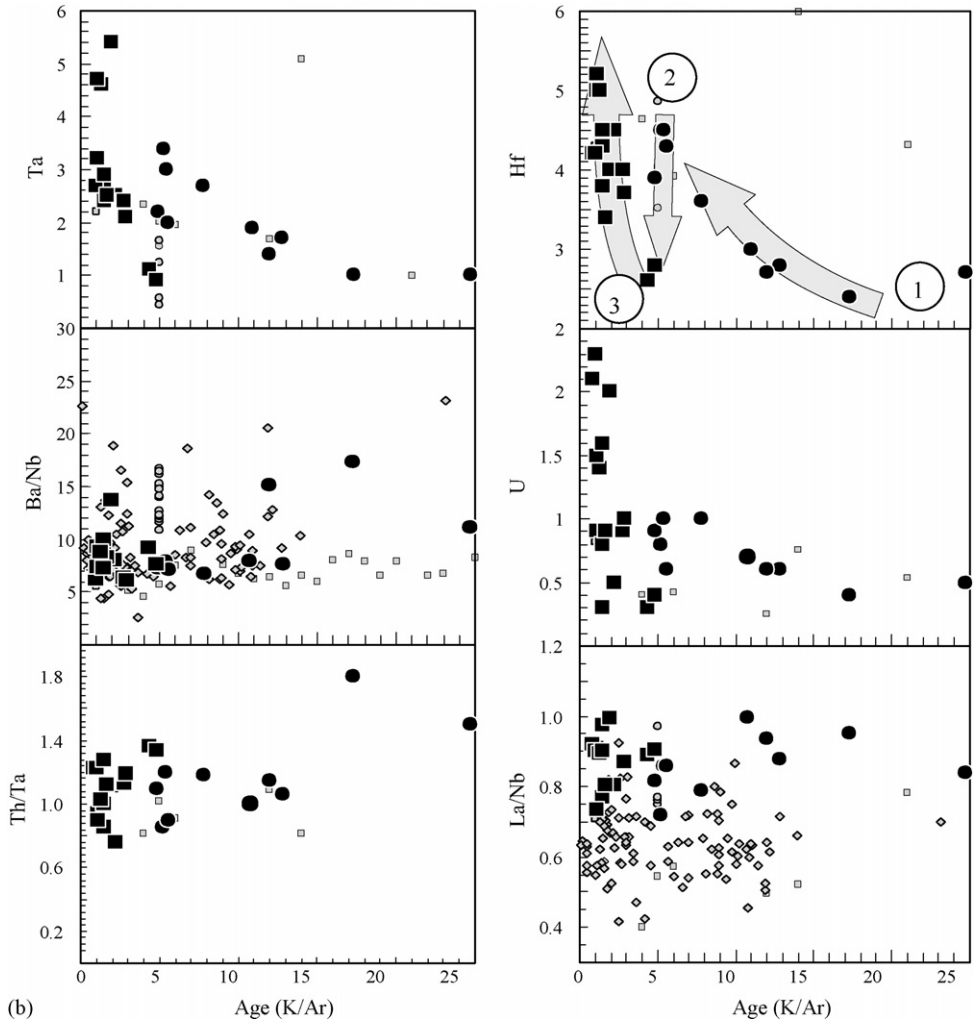

Fig. 10. (*Continued*).

Moreover, Zanchi et al. (2002) evidence the development of Pliocene N–S normal faults crossing the folds, testifying to a change in plate kinematics. This change in tectonic setting may have resulted in the abrupt geochemical change in magmas erupted at ∼5 Ma.

Another possible geological solution (not alternative to the first one) is a kinematic model proposed to solve the apparent paradox concerning the discrepancy in the amount of left-lateral offset between the southern and the northern segment of the DST. Indeed, the amount of left-lateral offset in the southern segment of the DST (i.e., south of Syria) is ∼105 km, whereas in the northern segment of the DST (i.e., in Lebanon and Syria) the offset is only ∼25 km (e.g., Chaimov et al., 1990; Zanchi et al., 2002; Rukieh et al., 2005; Sobolev et al., 2005). Baranzangi et al. (1993) proposed a two-step model: (1) during Miocene times (from ∼20 to ∼6 Ma) the southern DST segment probably continued north-westward to the actual location of the DST, along the Roum fault in the Mediterranean (Fig. 1); (2) only at the end of Miocene-beginning of Pliocene did the DST begin to propagate northward in Lebanon and Syria (the Yammouneh and El Ghab faults; Zanchi et al., 2002; Rukieh et al., 2005). This model can explain the discrepancy in the amount of left-lateral offset (together with about 20–30 km shortening occurred along the Palmyrides belt; Zanchi et al., 2002). Similarly, the development of the northern segment of the DST at the Miocene–Pliocene boundary could be considered the main cause of the abrupt change of composition of the Syrian lavas recorded at ∼5 Ma. A change of the structural regime at the end of Miocene is suggested by the development of pull-apart basins along the Yammouneh and El Ghab faults (e.g., Hula, Bokaieh and El Ghab basins) and the deepening of the Galilean basin (Heimann and Ron, 1993;

Hurwitz et al., 2002; Zanchi et al., 2002; Rukieh et al., 2005). Plio-Quaternary NW–SE oriented normal faults develop along the northern DST segment as extensional structures related to NS lateral shearing (Zanchi et al., 2002) favouring decompression melting of the upper mantle.

After the Arabia–Eurasia continental collision in middle–upper Miocene (e.g., Yilmaz et al., 1987), in NW Arabia a syn-collisional trans-tensional deformation occurred, with the development of the Hassa graben and Ceyhan–Osmaniye plain (Şengör, 1987; Polat et al., 1997).

In summary, the abrupt change in composition of the Syrian lavas at the Miocene–Pliocene boundary can be related to major plate re-organization which led to enhanced adiabatic melting as consequence of upper mantle decompression in a trans-tensional tectonic setting. Increasing degree of partial melting or shallower partial melting of upper mantle can, therefore, be a consequence of lithospheric movements during upper Neogene. LREE/HREE and MREE/HREE variation with age can be modelled according to this proposed scenario. Fig. 11 shows La/Yb and Gd/Yb ratios variation with age. At the Miocene–Pliocene boundary (grey field in Fig. 11) both ratios abruptly decrease as consequence of

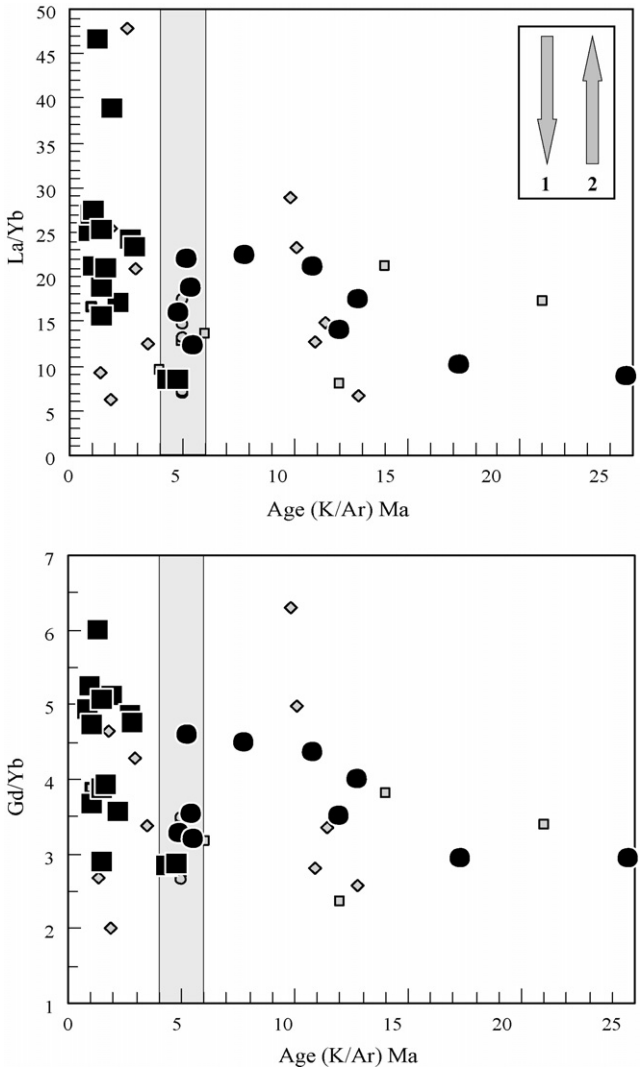

Fig. 11. La/Yb vs. age and Gd/Yb vs. age diagrams. Black circles = Syrian samples older than ~5 Ma. Black squares = Syrian samples younger than ~5 Ma. Arrow 1 = vector indicating qualitative effects of (a) increasing degree of partial melting and/or (b) increasing content of spinel in lherzolitic source. Arrow 2 = vector indicating qualitative effects of fractional crystallization of basaltic melts. At the Miocene–Pliocene boundary (grey field) an abrupt decrease of both LREE/HREE (La/Yb) and MREE/HREE (Gd/Yb) is evident. This change can be explained by an increasing degree of partial melting or by partial melting of shallower sources. The increase of both La/Yb and Gd/Yb ratios with decreasing age can be explained with fractional crystallization processes.

Table 2
Partition coefficients used in Fig. 12 to calculate the composition of partial melts from lherzolitic sources with variable spinel/garnet ratios

	Source	Distribution coefficients used in Fig. 12				
	Lith. M.	Ol	Opx	Cpx	Gt	Sp
La	2.6	0.0004[a]	0.002[a]	0.054[a]	0.01[a]	0.01[a]
Y	4.4	0.0125[b]	0.18[d]	0.467[f]	2.8[h]	0.008[l]
Yb	0.26	0.0015[a]	0.049[a]	0.28[a]	4.03[a]	0.01[a]
Sc	12.2	0.25[c]	0.857[e]	3[g]	4.7[i]	0.0478[m]

Lithospheric mantle estimates of McDonough (1990). References: (a) McKenzie and O'Nions (1991); (b) Kennedy et al. (1993); (c) Beattie (1994); (d) Green et al. (1989); (e) Colson et al. (1988), average value; (f) Hart and Dunn (1993); (g) Villemant et al. (1981); (h) Johnson (1994); (i) Jenner et al. (1993), average value; (l) assumed; (m) Nagasawa et al. (1980).

increasing degrees of partial melting and/or shallower depths of partial melting (i.e., increasing percentage of spinel in lherzolitic mantle).

8.5. Constraints on the mineralogy of mantle sources

It is important to constrain the paragenesis of Syrian lavas especially to identify the peridotite facies (i.e., spinel- or garnet-bearing) for the magma source. Two petrological models for the origin of the Cenozoic volcanism in Mashrek have been proposed: the first relates the igneous activity in this area to a north-westward channelling of the Afar mantle plume, and thus imply deep mantle sources (i.e., garnet-bearing peridotitic source(s); Camp and Roobol, 1992; Ilani et al., 2001; Sobolev et al., 2005), the second model proposes that the origin of magmatism is related to passive ascent of shallow lithospheric mantle, perhaps associated with the DST, linked with the opening of the Red Sea (i.e., spinel-bearing peridotitic source; Ibrahim et al., 2003; Shaw et al., 2003; Weinstein et al., 2006). Other intermediate models like the fossil-plume head model of Stein and Hofmann (1992) or a sort of finger-like small plumes model of Garfunkel (1989) have been proposed.

Fig. 12 shows La/Y versus Y and Sc/Yb versus Yb plots representing semi-quantitative geochemical modelling aimed to constrain the main Al-bearing phase in the mantle sources of the more primitive (i.e., MgO > 8 wt.%) Syrian lavas. The approach can be considered only semi-quantitative because several assumptions (e.g., the composition of the source, the abundance of minerals in the starting assemblage and in the residuum, the type of partial melting, the assumed partition coefficients and so on) have been chosen *ad hoc* and cannot be verified. In particular, the mantle source of the Syrian lavas has been supposed to be geochemically similar to the lithospheric mantle composition estimated by McDonough (1990). The olivine/clinopyroxene/orthopyroxene/(spinel, garnet) mode of the source is 0.60/0.09/0.25/0.06, respectively. The composition of the residual assemblage [the P value in the classical Shaw (1970) equation] has been set equal to −0.10/0.30/0.50/0.30 for olivine/clinopyroxene/orthopyroxene/(spinel, garnet). Partition coefficients used in the model for olivine, clinopyroxene, orthopyroxene, spinel and garnet are listed in Table 2. The equation used is the batch melting of Shaw (1970): $C_l = C_0/(D + F^*1 - P)$, where C_l is the concentration of element in the liquid, C_0 the concentration of the element in the starting assemblage; D the bulk distribution coefficient in the starting assemblage and P is the bulk distribution coefficient in the residuum. The results shown in Fig. 12 indicate that the less differentiated Syrian lavas (those with MgO > 8 wt.%) can be produced by relatively high degrees of melting ranging from ∼4 to ∼15% of a peridotitic assemblage with variable garnet/(spinel + garnet) ratio (ranging from 0.1 to 0.8). If these results are considered reliable, they indicate an upper asthenosphere mantle source (or lowermost lithospheric mantle source), since the spinel/garnet transition occurs nearly at 80–90 km depth, more or less the transition between lithosphere and asthenosphere (∼70–80 km; Hofstetter and Bock, 2004). These conclusions are in agreement with those of other investigations that proposed for all the Phanerozoic basalts from Arabia a lithospheric mantle source (Stein and Goldstein, 1996; Stein et al., 1997; Weinstein, 2000; Weinstein et al., 2006).

8.6. Origin of igneous activity in Syria

Several studies have proposed the existence of anomalous hot mantle beneath Mashrek to explain the volcanic activity. Weinstein et al. (2006) proposed for the origin of Israeli basalts a lithospheric mantle melting "caused by heat

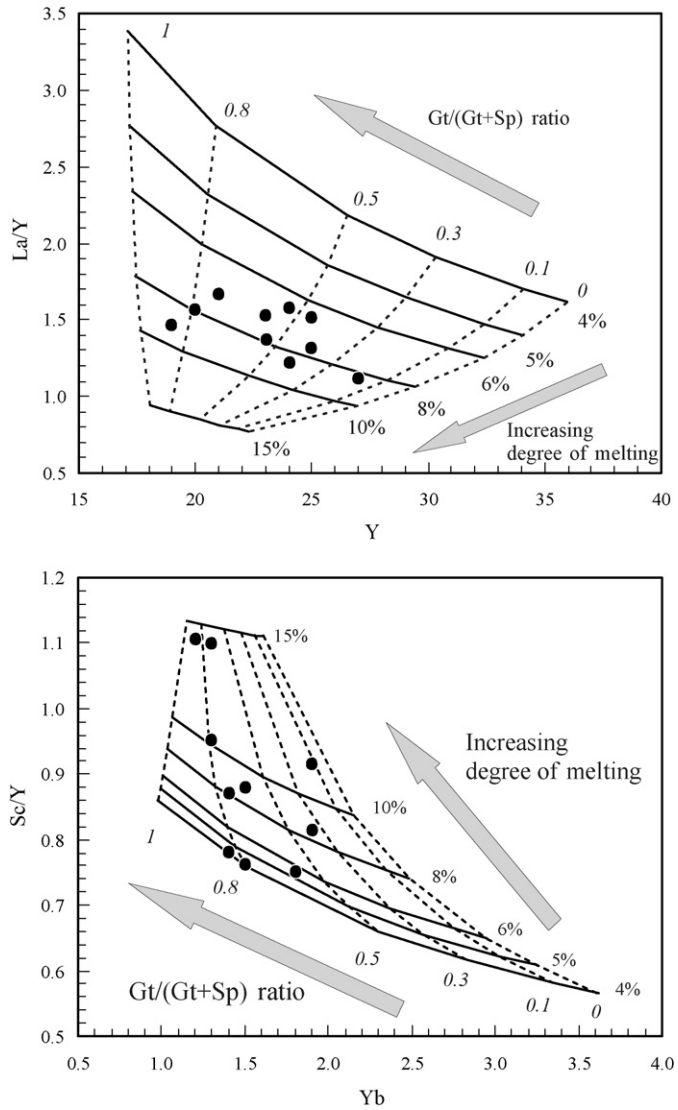

Fig. 12. La/Y vs. Y and Sc/Y vs. Yb diagrams. Only Syrian samples with MgO > 8 wt.% have been plotted. See Table 2 for parameters used and for references.

transferred by conduction from thermally anomalous zone within the sub-lithospheric mantle". Their model shows some similarities with the model of Garfunkel (1989) who proposed that the Cenozoic magmatism in the Arabian plate could be related to the existence of "several short-lived upwellings which formed intermittently beneath a wide region". Moreover, Garfunkel (1989) considered improbable any genetic relationship between the volcanic activity of the Harrat Ash Shaam and that developed along the DST. The main difference between the models of Weinstein et al. (2006) and Garfunkel (1989) is that the firsts consider only heat transfer from sub-lithospheric depths, whereas Garfunkel (1989) proposes also mass transfer from asthenospheric or deeper sources. Stein and Hofmann (1992) linked the relative homogeneity of Phanerozoic basalts of the Arabian plate in terms of Sr–Nd isotopic ratios to a common mantle source, represented by a fossil plume head attached to the base of the Arabian lithosphere since the Proterozoic. All these models are based on the assumption of the existence of a sub-lithospheric mantle hotter than normal. The source of this hot mantle could be either a large fossil plume head or smaller, finger-like instabilities like those proposed for other circum-Mediterranean anorogenic volcanic rocks (e.g., Wilson and Patterson, 2001; Lustrino and Wilson, in press; Lustrino and Carminati, submitted for publication).

Differently from the above models (that considered unlike any relation between Cenozoic volcanism in Arabia and the Afar mantle plume), Sobolev et al. (2005) proposed for the igneous activity along the DST a direct link with Afar. Their conclusions are based on the asymmetric topography along the DST, with the eastern shoulder being more elevated (up to 1500 m in altitude) compared to the western shoulder (~500 m in altitude; see their Fig. 6). Sobolev et al. (2005) related this asymmetric topography to a mechanical coupling of the western shoulder of the DST to the cold (and therefore dense) Mediterranean (Levantine) lithosphere, whereas the eastern shoulder is uplifted as consequence of the presence of hot (and therefore buoyant) mantle, heated by the Arabian shield mantle adjacent to the DST (i.e., presence of anomalously hot mantle = mantle plume).

The asymmetric topography is a main feature of the entire Dead Sea–Red Sea zone. In particular, the difference in topography across the Read Sea (with several hundred of meters of altitude difference between the Egyptian and the Arabian shoulder) has been elegantly modelled by Doglioni et al. (2003) as consequence of isostatic causes not requiring anomalously hot mantle beneath the Arabian plate. The Doglioni et al. (2003) model is based on a worldwide evidence that oceanic ridges and continental rift zones are more elevated along the eastern side. These authors explain this asymmetry by the horizontal motion (W-directed) of the lithospheric mantle with respect to asthenospheric mantle (with a relative E-directed motion) from which it is decoupled. As a result, during continental rift (or in trans-tensional settings) the mantle beneath the eastern side of the rift is more depleted (and therefore less dense, having lost most of its original Fe) than the mantle beneath the western side (still relatively "primitive"). According to this model, no heat anomalies are required to explain the higher topography of the eastern shoulder of the Red Sea. The Doglioni et al. (2003) model cannot be directly translated to the Dead Sea Transform zone (because along this fault the magmatic activity is only minor) but what is important to keep in mind is that differences of altitude can be related to isostatic causes with lithospheric mantles variably depleted (i.e., variably dense and therefore variably buoyant).

The new data on Syrian basalts presented in this paper can be used to propose a petrogenetic model for the Neogene volcanic rocks of Syria and the entire Mashrek. Here we propose that lithospheric extension is the main cause of igneous activity in Syria. The role of deep-rooted mantle plumes is considered inconsistent with several lines of evidence: (a) most of the magmatism in northern Mashrek segment is concentrated along the DST and generally post-dates the development of the fault (e.g., Garfunkel, 1989). Moreover, Litak et al. (1997) noted that most of the Neogene volcanic activity on the northern Arabian plate shows north-westerly striking volcanic vents aligned along the Najd fault system (a Pan-African orogeny-related strike-slip fault zone; e.g., Beydoun, 1991). These observations may be interpreted as a strong structural control by lithospheric discontinuities representing preferential pathways for uprising magmas; (b) the composition of the most primitive magmas is thought to be in equilibrium with a spinel-bearing or spinel-garnet-bearing lherzolitic assemblage (Fig. 12), thus constraining the depth of origin to the lowermost lithospheric mantle or the uppermost asthenosphere (i.e., shallow mantle); (c) the heat flux in the Mashrek area is low to very low (around 1 HFU, even close to the DST; Ben-Avraham et al., 1978; Eckstein and Simmons, 1979; Forster et al., 2004), thus arguing against anomalously hot mantle sources; (d) much of the uplift along the DST developed after the beginning of the igneous activity (more than 70% of the uplift is younger than ~5 Ma; Ginat et al., 2000; Gomez et al., 2006); (e) the absence of a systematic age progression of magmatic activity speaks for different igneous activity in different places in the Mashrek, thus reinforcing the idea that this activity cannot be related neither to a deep mantle plume neither to a mantle plume channelling coming from SE (Afar); (f) the length of the volcanic activity developed in Syria and Mashrek (>25 Ma, probably > 40 Ma) is much longer than typical time intervals of volcanism in localities where a deep mantle plume is supposed to have impinged beneath the lithosphere (e.g., <5 Ma, generally 1–2 Ma); (g) major and trace element similarities between Cenozoic volcanic rocks from Syria and for the rest of the products related to the circum-Mediterranean Anorogenic Cenozoic Igneous Province (Lustrino, 2003; Lustrino and Wilson, in press) argue for a relatively common shallow mantle sources throughout the Mediterranean Sea and neighbouring areas (the CMR, Common Magmatic Reservoir of Lustrino and Wilson, in press); (h) several petrological studies dealing with Sr–Nd–Pb–Hf–He isotopic considerations (e.g., Bertrand et al., 2003; Shaw et al., 2003) considered very improbable any involvement of the Afar plume in the genesis of volcanic rocks from central–northern Arabia (i.e., Mashrek area).

9. Concluding remarks

An extensive volcanic activity developed from the Upper Eocene to Holocene (~40–0.0005 Ma) in the Mashrek Region. The magmatism occurs along the western Arabian plate, mostly east of the Dead Sea Transform fault, a sinistral strike-slip fault running from the Gulf of Aquaba in the Red Sea to the fold structures of Taurides (Anatolia) for a

total length of about 1000 km and up to 105 total displacement. About 95% of the published age determinations are <20 Ma, suggesting that most of the volcanic activity is confined to Miocene-Quaternary times.

The age of the basaltic samples from western Syria range from ~25 to ~1 Ma, with 20 out 26 analyses younger than 5.5 Ma. The samples are mostly high TiO_2 alkaline mafic rocks plus rare transitional/tholeiitic basalts and basaltic andesites. Major and trace element content of the Syrian lavas plot within the field of the other Mashrek Cenozoic igneous rocks, allowing the hypothesis of a common origin for the Cenozoic anorogenic magmatism of the entire circum-Mediterranean area (the so-called Common Magmatic Reservoir; Lustrino and Wilson, in press). Sr and Nd isotopes of Syrian lavas show many similarities with the rest of the Mashrek basalts, with the exception of Israeli rocks, characterized by nearly constant lower $^{87}Sr/^{86}Sr$ for a given $^{143}Nd/^{144}Nd$.

Semi-quantitative geochemical modelling on the most primitive lavas of Syria evidence a composition in equilibrium with a mixed spinel-garnet composition that has suffered variable degrees of partial melting ranging from ~6 to ~15%.

A major change in plate kinematics recorded at the Miocene–Pliocene boundary (as evidenced by structural, geological, paleogeographic and sedimentological studies) is here considered at the base of the abrupt change in composition of the Syrian lavas recorded at ~4.9 Ma. The transition from strongly compressive to trans-tensional stresses may have allowed major partial melting as consequence of upper mantle decompression, mostly along the DST. Partial melts of upper mantle followed minor fractionation at mantle levels.

Several considerations allow an interpretation of the origin of the igneous activity in Syria (as well as in other Mashrek localities) being unrelated to local deep mantle plumes or to the Afar plume: (1) most of the magmatism is concentrated along the DST, therefore it implies a strong lithospheric control on the locus of upper mantle partial melting; (2) the spinel/garnet-bearing lherzolitic source evidenced by semi-quantitative geochemical modelling can be related only to relatively shallow sources (i.e., generally <90 km in depth); (3) the low heat flux measured in the north Arabian plate is in contrast with the presence of heat anomaly as instead requested by the mantle plume model; (4) most of the magmatism post-dates the development of the DST and the relatively strong uplift develops after or during the last stages of magmatism; (5) no age progression of magmatic activity has been recorded in Syria and the entire Mashrek; (6) the long time span of volcanic activity in Syria and in Mashrek in general (~20–40 Ma) is distinct from the length of volcanic activities believed related to deep mantle plumes (~1–2 Ma); (7) the gross major and trace element similarity, as well as Nd isotopic ratios, with the other circum-Mediterranean Anorogenic Cenozoic Igneous Province can be interpreted as a feature related to a relatively common shallow mantle (upper asthenosphere) origin, without requiring any presence of deeply rooted mantle plumes; (8) subtle but clear geochemical differences, in particular in Sr and Pb isotopic ratios, between Afar plume-related magmas (e.g., Cenozoic volcanic rocks from Djibuti, Yemen and Ethiopia) and the rest of the volcanic rocks from central–northern Arabia argue against any direct or indirect derivation of the volcanism in Mashrek from the Afar plume.

Acknowledgements

The first author thanks Maria Luisa Libutti and Gabriella Pintucci (Rome) for their professional help in accessing the literature papers, and to Alessio Carminati's parents for their logistic assistance during the writing of the first draft this manuscript. Special thanks also to Fred Frey (Boston, USA) for useful comments on an early draft of this manuscript and for English text checking. Discussion of ML with Eugenio "break-off" Carminati (Rome) and Carlo "mantle-push" Doglioni (Rome) improved this manuscript. ES thanks A.E. Dodonov (Moscow, Russia) and Samir Hanna (Damascus, Syria) for help in carrying out field geological investigations and sampling. Brian Cousens (Ottawa, Canada) and an anonymous referees are thanked for their useful suggestions. This research was supported by MIUR (FIRB 2001 and PRIN 2004) and University La Sapienza (ex 60% 2003 and 2004) grants to ML. The first author wishes to express the warmest thanks to Enrica, Bianca and Laura for their patience during the writing of this manuscript and to Robert Plant, Jimmy Page, John Paul Jones and John "Bonzo" Bonam for their "black dog".

References

Abdel-Rahman, A.-F.M., 2002. Mesozoic volcanism in the Middle East: geochemical, isotopic and petrogenetic evolution of extension-related alkali basalts from central Lebanon. Geol. Mag. 139, 621–640.

Abdel-Rahman, A.-F.-M., Nassar, Ph.E., 2004. Cenozoic volcanism in the Middle East: petrogenesis of alkali basalts from northern Lebanon. Geol. Mag. 141, 545–563.

Aksu, A.E., Hall, J., Yaltirak, C., 2005. Miocene to recent tectonic evolution of the eastern Mediterranean: new pieces of the old Mediterranean puzzle. Mar. Geol. 221, 1–13.

Al-Saad, D., Sawaf, T., Gebran, A., Barazangi, M., Best, J., Chiamov, T., 1992. Crustal structure of central Syria, the intracontinental Palmyride mountain belt. Tectonophysics 207, 345–358.

Altherr, R., Henjes-Kunst, F., Baumann, A., 1990. Asthenosphere versus lithosphere as possible sources for basaltic magmas erupted during formation of the Red Sea: constraints from Sr, Pb and Nd isotopes. Earth Planet. Sci. Lett. 96, 269–286.

Alici, P., Temel, A., Gourgaud, A., Vidal, Ph., Nyazi Gundogdu, M., 2001. Quaternary tholeiitic to alkaline volcanism in the Karasu valley, Dead Sea rift zone, southeast Turkey: Sr–Nd–Pb–O isotopic and trace-element approaches to crust-mantle interaction. Int. Geol. Rev. 43, 120–138.

Baker, J.A., Menzies, M.A., Thirlwall, M.F., MacPherson, C.G., 1997. Petrogenesis of Quaternary intraplate volcanism, Sana'a, Yemen: implications for plume-lithosphere interaction and polybaric melt hybridization. J. Petrol. 36, 1359–1390.

Baranzangi, M., Seber, D., Chaimov, T., Best, J., Litak, R.D., Sawaf, T., 1993. Tectonic evolution of the northern Arabian plate in western Syria. In: Boschi, E., Mantovani, E., Morelli, A. (Eds.), Recent Evolution and Seismicity of the Mediterranean Region. Kluwer Academic Publishers, Dordrecht, The Netherlands, pp. 117–140.

Barberi, F., Capaldi, G., Gasperini, P., Marinelli, G., Santacroce, R., Scandone, R., Treuil, M., Varet, J., 1979. Recent basaltic volcanism of Jordan and its implications on the geodynamic history of the Dead Sea shear zone. Acc. Naz. Lincei, Atti dei Convegni 47, 667–683.

Beattie, P., 1994. Systematics and energetics of trace-element partitioning between olivine and silicate melts: implications for the nature of mineral/melt partitioning. Chem. Geol. 117, 57–71.

Beccaluva, L., Bianchini, G., Wilson, M. (Eds.). Cenozoic magmatism in the Mediterranean area. Geol. Soc. Am. Spec. Vol., in press.

Ben-Avraham, Z., Ginzburg, A., 1990. Displaced terranes and crustal evolution of the Levant and eastern Mediterranean. Tectonics 9, 613–622.

Ben-Avraham, Z., Haenel, R., Villinger, H., 1978. Heat flow through the Dead Sea rift. Mar. Geol. 28, 253–269.

Bertrand, H., Chazot, G., Blichert-Toft, J., Thoral, S., 2003. Implications of widespread high-μ volcanism on the Arabian Plate for Afar mantle plume and lithosphere composition. Chem. Geol. 198, 47–61.

Best, J.S., Barazangi, M., A.-Saad, D., Sawaf, T., Gebran, A., 1990. Bouguer gravity trends and crustal structure of the Palmyride Mountain belt and surrounding northern Arabian platform in Syria. Geology 18, 1235–1239.

Beydoun, Z.R., 1991. Arabian plate hydrocarbon geology and potential – a plate tectonic approach. Am. Assoc. Petrol. Geol. Stud. Geol., 33.

Bilal, A., Touret, J.L.R., 2001. Les enclaves du volcanisme récent du rift syrien. Bull. Soc. Géol. Fr. 172, 3–16.

Camp, V.E., Roobol, J.M., 1989. The Arabian continental alkali basalt province. Geol. Soc. Am. Bull. 101, 71–95.

Camp, V.E., Roobol, J.M., 1992. Upwelling asthenosphere beneath western Arabia and its regional implications. J. Geophys. Res. 97, 15255–15271.

Çapan, U.Z., Vidal, Ph., Cantagrel, J.M., 1987. K–Ar, Nd, Sr and Pb isotopic study of Quaternary volcanism in Karasu Valley (Hatav), N-end of Dead-Sea Rift zone in SE Turkey. Yerbilimleri 14, 165–178.

Chaffey, D.J., Cliff, R.A., Wilson, B.M., 1989. Characterization of the St. Helena magma source magmatism in the ocean basins. In: Saunders, A.D., Norry, M.J. (Eds.), Geol. Soc. Lond., London, 257–276.

Chaimov, T., Barazangi, M., Al.Saad, D., Sawaf, T., Gebran, A., 1990. Crustal shortening in the Palmyride fold belt, Syria, and implications for movement along the Dead Sea fault system. Tectonics 9, 1369–1386.

Colson, R.O., McKay, G.A., Taylor, L.A., 1988. Temperature and composition dependencies of trace element partitioning: Olivine/melt and low-Ca pyroxene/melt. Geochim. Cosmochim. Acta 52, 539–553.

Doglioni, C., 1995. Geological remarks on the relationships between extension and convergent geodynamic settings. Tectonophysics 252, 253–267.

Doglioni, C., Carminati, E., Monatti, E., 2003. Rift asymmetry and continental uplift. Tectonics 22 (3), 1024, doi:10.1029/2002TC001459.

Eckstein, Y., Simmons, G., 1979. Review of heat flow data from the eastern Mediterranean region. Pure Appl. Geophys. 117, 150–159.

Fediuk, F., Al Fugha, H., 1999. Dead sea region: fault-controlled chemistry of Cenozoic volcanics. Geolines 9, 29–34.

Forster, H.-J., Forster, A., Oberhansli, R., Stromeyer, D., Sobolev, S.V., 2004. Lithosphere composition and thermal regime across the Dead Sea Transform in Israel and Jordan. CGU-AGU-SEG-EEGS 2004 Joint Assembly, Montreal (CD-ROM Y11 A-05).

Garfunkel, Z., 1981. Internal structure of the Dead Sea leaky transform (rift) in relation to plate kinematics. Tectonophysics 80, 81–108.

Garfunkel, Z., 1989. Tectonic setting of Phanerozoic magmatism in Israel. Isr. J. Earth Sci. 38, 51–74.

Giannérini, G., Campredon, R., Féraud, G., Abou, Zakhem, B., 1988. Déformations intraplaques et volcanisme associé: exemple de la bordure NW de la plaque arabique au Cénozoique. Bull. Soc. Geol. Fr. 8, 937–947.

Ginat, H., Zilberman, E., Avni, Y., 2000. Tectonic and paleogeographic significance of the Edom River, a Pliocene stream that crossed the Dead Sea rift valley. Isr. J. Earth Sci. 49, 159–177.

Gomez, F., Khawlie, M., Tabet, C., Nasser, Darkal, A., Khair, K., Barazangi, M., 2006. Late Cenozoic uplift along the northern Dead Sea transform in Lebanon and Syria. Earth Planet. Sci. Lett. 241, 913–931.

Green, T.H., Sie, S.H., Ryan, C.G., Cousens, D.R., 1989. Proton microprobe-determined partitioning of Nb, Ta, Zr, Sr and Y between garnet, clinopyroxene and basaltic magma at high pressure and temperature. Chem. Geol. 74, 201–216.

Hall, J., Aksu, A.E., Calon, T.J., Yasa, r, D., 2005. Varying tectonic control on basin development at an active microplate margin: Latakia Basin. East. Mediterr. Mar. Geol. 221, 15–60.

Hart, S.R., Dunn, T., 1993. Experimental cpx/melt partitioning of 24 trace elements. Contrib. Mineral. Petrol. 113, 1–8.

Hegner, E., Pallister, J.S., 1989. Pb, Sr and Nd isotopic characteristics of Tertiary Red Sea volcanics from the central Saudi Arabian coastal plain. J. Geophys. Res. 94, 7749–7755.

Heimann, A., Ron, H., 1993. Geometric changes of plate boundaries along part of the northern Dead Sea transform: geochronologic and paleomagnetic evidence. Tectonics 12, 477–491.

Heimann, A., Steinitz, G., 1988. K-Ar ages of basalts from the western slopes of the Golan Heights. Geol. Surv. Israel Curr. Res. 6, 29–32.

Hofmann, A.W., Jochum, K.P., Seufert, M., White, W.M., 1988. Nb and Pb in oceanic basalts: new constraints on mantle evolution. Earth Planet. Sci. Lett. 79, 33–45.

Hofstetter, A., Bock, G., 2004. Shear-wave velocity structure of the Sinai sub-plate from receiver function analyses. Geophys. J. Int. 158, 67–84.
Hurwitz, S., Garfunkel, Z., Ben-Gai, Y., Reznikov, M., Rotstein, Y., Gvirtzman, H., 2002. The tectonic framework of a complex pull-apart basin: seismic reflection observations in the Sea of Galilee, Dead Sea transform. Tectonophysics 359, 289–306.
Ibrahim, K.M., Tarawneh, K., Rabba, I., 2003. Phases of activity and geochemistry of basaltic dike systems in northeast Jordan parallel to the Red Sea. J. Asian Earth Sci. 21, 467–472.
Ilani, S., Harlavan, Y., Tarawneh, K., Rabba, I., Weinberger, R., Ibrahim, K., Peltz, S., Steinitz, G., 2001. New K-Ar ages of basalts from the Harrat Ash Shaam volcanic field in Jordan: implications for the span and duration of the upper-mantle upwelling beneath the western Arabian plate. Geology 29, 171–174.
Irvine, T.N., Baragar, R.A.W., 1971. A guide to the chemical classification of the common volcanic rocks. Can. J. Earth Sci. 8, 523–547.
Jenner, G.A., Foley, S.F., Jackson, S.E., Green, T.H., Fryer, B.J., Longerich, H.P., 1993. Determination of partition coefficients for trace elements in high pressure-temperature experimental run products by laser ablation microprobe-inductively coupled plasma mass spectrometry (LAM-ICP-MS). Geochim. Cosmochim. Acta 57, 5099–5103.
Johnson, K.T.M., 1994. Experimental cpx/ and garnet/melt partitioning of REE and other trace elements at high pressures: petrogenetic implications. Miner. Mag. 58, 454–455.
Kennedy, A.K., Lofgren, G.E., Wasserburg, G.J., 1993. An experimental study of trace element partitioning between olivine, orthopyroxene and melt in chondrules: equilibrium balues and kinetic effects. Earth Planet. Sci. Lett. 115, 177–195.
Khair, K., Tsokas, G.N., 1999. Nature of the Levantine (eastern Mediterranean crust from multiple-source Werner deconvolution of Bouger gravity anomalies. J. Geophys. Res. 104, 25469–25478.
Kogarko, L.N., Asavin, A.M., Barsikov, V.L., Kolesov, G.M., Kruchkova, O.I., Polyakov, A.I., Ramendik, G.I., 1984. A geochemical model for rare-earth fractionation in alkali-basalt series in South Atlantic islands. Geochem. Int. 21, 27–39.
Laws, E.D., Wilson, M., 1997. Tectonics and magmatism associated with Mesozoic passive continental margin development in the Middle East. J. Geol. Soc. Lond. 154, 757–760.
Le Bas, M.J., le Maitre, R.W., Streckeisen, A., Zanettin, B., 1986. A chemical classification of volcanic rocks based on the total alkali-silica diagram. J. Petrol. 27, 745–750.
LePichon, X., Gaulier, J.M., 1988. The rotation of Arabia and the Levant fault system. Tectonophysics 153, 271–294.
Litak, R.K., Barazangi, M., Beauchamp, W., Seber, D., Brew, G., Sawaf, T., Al-Youssef, W., 1997. Mesozoic-Cenozoic evolution of the intraplate Euphrates fault system Syria: implications for regional tectonics. J. Geol. Soc. Lond. 154, 653–666.
Lustrino, M., 2000. Volcanic activity during the Neogene to present evolution of the western Mediterranean area: a review. Ofioliti 25, 87–101.
Lustrino, M., 2003. Spatial and temporal evolution of Cenozoic igneous activity in the circum-Mediterranean realm. Inst. Geophys. Polish Acad. Sci. M-28 (363), 143–144.
Lustrino, M., Carminati, E. Phantom plumes in old Europe. In: Foulger, G.R., Jurdy, D.M. (Eds.), The origins of melting anomalies: Plumes, Plates and Planetary Processes. Geol. Soc. Am. Spec. Paper., submitted for publication.
Lustrino, M., Wilson, M. The circum-Mediterranean Anorogenic Cenozoic Igneous Province. Earth Sci. Rev., in press.
Lustrino, M., Melluso, L., Morra, V., 2002. The transition from alkaline to tholeiitic magmas: a case study from the Orosei-Dorgali Pliocene volcanic district (NE Sardinia Italy). Lithos 63, 83–113.
Lustrino, M., Melluso, L., Morra, V. The geochemical peculiarity of "Plio-Quaternary" volcanic rocks of Sardinia in the circum-Mediterranean area. In: Beccaluva, L., Bianchini, G., Wilson, M. (Eds.), Cenozoic Magmatism in the Mediterranean Area. Geol. Soc. Am. Spec. Paper, in press.
McClusky, S., Reilinger, R., Mahmoud, S., Ben Sari, D., Taeleb, A., 2003. GPS constraints on Africa (Nubia) and Arabia plate motions. Geophys. J. Int. 155, 126–138.
McDonough, W.F., 1990. Constraints on the composition of the continental lithospheric mantle. Earth Planet. Sci. Lett. 101, 1–18.
McDonough, W.F., Sun, S.-S., 1989. The composition of the Earth. Chem. Geol. 120, 223–253.
McKenzie, D., O'Nions, R.K., 1991. Partial melt distributions from inversion of rare earth element concentratjions. J. Petrol. 32, 1021–1091.
Miller, D.M., Goldstein, S.L., Langmuir, C.H., 1994. Cerium/lead and lead isotope ratios in arc magmas and the enrichment of lead in the continents. Nature 368, 514–520.
Mittlefehldt, D.W., 1984. Genesis of cpx-amphibole xenoliths from Birket Ram: trace element and petrologic constraints. Contrib. Mineral. Petrol. 88, 280–287.
Mor, D., 1993. A time-table for the Levant Volcanic Province, according to K-Ar dating in the Golan Heights. Isr. J. Afr. Earth Sci. 16, 223–234.
Mouty, M., Delaloye, M., Fontignie, D., Piskin, O., Wagner, J.J., 1992. The volcanic activity in Syria and Lebanon between Jurassic and actual. Schweiz. Miner. Petr. Mitt. 72, 91–105.
Nagasawa, H., Schreiber, H.D., Morris, R.V., 1980. Experimental mineral/liquid partition coefficients of the rare earth elements, Sc and Sr for perovskite, spinel and melilite. Earth Planet. Sci. Lett. 46, 431–437.
Nasir, S., Safarjalani, A., 2000. Lithospheric petrology beneath the northern part of the Arabian plate in Syria: evidence from xenoliths in alkali basalts. J. Afr. Earth Sci. 30, 149–168.
Netzeband, G.L., Gohl, K., Hubscher, C.P., Ben-Avraham, Z., Dehghani, G.A., Gajewski, D., Liersch, P., 2006. The Levantine Basin – crustal structure and origin. Tectonophysics 418, 167–188.
Newsom, H.E., White, W.M., Jochum, K.P., Hofmann, A.W., 1986. Siderophile and chalcophile element abundances in oceanic basalts, Pb isotope evolution and growth of the Earth's core. Earth Planet. Sci. Lett. 80, 299–313.
Omar, G.I., Steckler, M.S., 1995. Fission track evidence on the initial rifting of the Red Sea: two pulses, no propagation. Science 270, 1341–1344.
Polat, A., Kerrich, R., Casey, J.F., 1997. Geochemistry of Quaternary basalts erupted along the East Anatolian and Dead Sea fault zones of southern Turkey: implications for mantle sources. Lithos 40, 55–68.
Rukieh, M., Trifonov, V.G., Dodonov, A.E., Minini, H., Ammar, O., Ivanova, T.P., Zaza, T., Ysef, A., Al-Shara, M., Jobaili, Y., 2005. Neotectonic map of Syria and some aspects of Late Cenozoic evolution of the northwestern boundary zone of the Arabian plate. J. Geodyn. 40, 135–256.

Salel, J.F., Seguret, M., 1994. Late Cretaceous to Paleogene thin-skinned tectonics of the Palmyrides belt (Syria). Tectonophysics 234, 265–290.
Şengör, A.M.C., 1987. Tectonic of Tethysides: orogenic collage development in a collisional setting. Annu. Rev. Earth Planet. Sci. 15, 213–244.
Sharkov, E.V., Chernyshev, I.V., Devyatkin, E.V., Dodonov, A.E., Ivanenko, V.V., Karpenko, M.I., Lebedev, V.A., Novikov, V.M., Hanna, S., Khatib, K., 1998. New data on the geochronology of upper Cenozoic plateau basalts from the northeastern periphery of the Red Sea rift area (northern Syria). Dodlady Earth Sci. 358, 19–22.
Sharkov, E.V., Chernyshev, I.V., Devyatkin, E.V., Dodonov, A.E., Ivanenko, V.V., Karpenko, M.I., Leonov, Y.G., Novikov, V.M., Hanna, S., Khatib, K., 1994. Geochronology of late Cenozoic basalts in western Syria. Petrology 2, 385–394.
Sharkov, E.V., Snyder, G.A., Taylor, L.A., Laz'ko, E.E., Jerde, E., Hanna, S., 1996. Geochemical peculiarities of the asthenosphere beneath the Arabian plate: evidence from mantle xenoliths of the Quaternary Tell-Danun volcano (Syrian-Jordan plateau, southern Syria). Geochem. Int. 34, 737–752.
Shaw, D.M., 1970. Trace element fractionation during anatexis. Geochim. Cosmochim. Acta 34, 237–243.
Shaw, J.E., Baker, J.A., Menzies, M.A., Thirlwall, M.F., Ibrahim, K.M., 2003. Petrogenesis of the largest intraplate volcanic field on the Arabian Plate (Jordan): a mixed lithosphere–asthenosphere source activated by lithospheric extension. J. Petrol. 44, 1657–1679.
Sobolev, S.V., Petrunin, A., Garfunkel, Z., Babeyko, A.Y., 2005. Thermo-mechanical model of the Dead Sea Transform. Earth Planet. Sci. Lett. 238, 78–95.
Spera, F.J., 1984. Carbon dioxide in petrogenesis. III. Role of volatiles in the ascent of alkaline magma with special reference to xenolith-bearing mafic lavas. Contrib. Mineral. Petrol. 88, 217–232.
Stein, M., Goldstein, S.L., 1996. From plume head to continental lithosphere in the Arabian-Nubian shield. Nature 382, 773–778.
Stein, M., Hofmann, A.W., 1992. Fossil plume head beneath the Arabian lithosphere? Earth Planet. Sci. Lett. 114, 193–209.
Stein, M., Navon, O., Kessel, R., 1997. Chromatographic metasomatism of the Arabian–Nubian lithosphere. Earth Planet. Sci. Lett. 152, 75–91.
Sun, S.S., McDonough, W.F., 1989. Chemical and isotopic systematics of oceanic basalts: implications for mantle compositions and processes. In: Saunders, A.D., Norry, M.J. (Eds.), Magmatism in the Ocean Basins. Geol. Soc. Lond. Spec. Publ. 42, 313–345.
Thirlwall, M.F., 1997. Pb isotopic and elemental evidence for OIB derivation from young HIMU mantle. Chem. Geol. 139, 51–74.
Vauchez, A., Barruol, G., Tommasi, A., 1997. Why do continents break-up parallel to ancient orogenic belts? Terra Nova 9, 62–66.
Villemant, B., Jaffrezic, H., Joran, J.-L., Treuil, M., 1981. Distribution coefficients of major and trace elements; fractional crystalization in the alkali basalt series of Chaine des Puys (Massif Central France). Geochim. Cosmochim. Acta 45, 1997–2001.
Weaver, B.L., Wood, D.A., Tarney, J., Joron, J.-L., 1987. In: Fitton, J.G., Upton, B.G.J. (Eds.), Geochemistry of ocean island basalts from the South Atlantic, Ascension, Bouvet, St. Helena, Gough and Tristan da Cunha| alkaline igneous rocks. Geol. Soc. Lond., 253–267.
Weinstein, Y., 2000. Spatial and temporal geochemical variability in basin-related volcanism, northern Israel. J. Afr. Earth Sci. 30, 865–886.
Weinstein, Y., Navon, O., Altherr, R., Stein, M., 2006. The role of lithospheric mantle heterogeneity in the generation of Plio-Pleistocene alkali basaltic suites from NW Harrat Ash Shaam (Israel). J. Petrol. 47, 1017–1050.
Weinstein, Y., Navon, O., Lang, B., 1994. Fractionation of Pleistocene alkali basalts from the northern Golan Heights. Isr. J. Earth Sci. 43, 63–79.
Willbold, M., Stracke, A., 2006. Trace element composition of mantle end-members: implications for recycling of oceanic and upper and lower continental crust. Geochem. Geophys. Geosyst. 7 (4), doi:10.1029/2005GC001005.
Wilson, M., Bianchini, G., 1999. Tertiary–Quaternary magmatism within the Mediterranean and surrounding regions. In: Durand, B., Jolivet, L., Horvath, F., Seranne, M. (Eds.), The Mediterranean Basins: Tertiary Extension within the Alpine Orogen. Geol. Soc. Lond. 156, 141–168.
Wilson, M., Patterson, R., 2001. Intraplate magmatism related to short-wavelength convective instabilities in the upper mantle: evidence from the Tertiary-Quaternary volcanic province of western and central Europe. In: Ernst, R.E., Buchan, K.L. (Eds.), Mantle plumes: their identification through time, Geol. Soc. Am. Spec. Paper 352, 37–58.
Yilmaz, Y., Şaroğlu, F., Güner, Y., 1987. Initiation of the neomagmatism in East Anatolia. Tectonophysics 134, 177–199.
Zanchi, A., Crosta, G.B., Darkal, A.N., 2002. Paleostress analyses in NW Syria: constraints on the Cenozoic evolution of the northwestern margin of the Arabian plate. Tectonophysics 357, 255–278.